

# Master Thesis

## Civil Engineering & Management

Optimization of sheet pile designs for sand dikes

K. Singh s2586827

Daily supervisor  
UT supervisor  
External supervisor

dr. H. Cheng  
prof. dr. V. Magnanimo  
ir. K. ten Pas RC

May 5, 2025

UNIVERSITY  
OF TWENTE.

nepocon

## Summary

One of the failure mechanisms that can occur in dikes is outward macro-stability, commonly associated with slope sliding failure. This natural phenomenon is particularly present in sand dikes where erosion and washout of sand occur due to fluctuations in water levels. Mitigating this failure mechanism requires structural implementation. Sheet piles are commonly used structures to enhance the stability of dikes. However, installing sheet piles requires production, transportation, and construction activities which impacts sustainability and costs negatively. Therefore, sustainability and cost-efficiency aspects should be considered within the design and engineering phase.

Assessing geotechnical structures such as dikes can be effectively analyzed by using finite element analysis software, specifically PLAXIS. This software enables the configuration of different sheet pile designs to ensure the safety of the dike. However, the analysis of different sheet pile designs can be time-consuming by continuously adjusting input parameters manually. The incorporation of machine-learning tools can significantly improve this process. GrainLearning, a tool employed for uncertainty analysis and design optimization, allows the software to autonomously select input parameters based on design requirements, such as the factor of safety. This ability reduces repetitive work by the user and increases efficiency for practitioners at engineering firms.

In this research, the dike located near the pumping station in Terwolde, Netherlands, is used as a case study for the integration of the GrainLearning tool with PLAXIS. Initially, a finite element model is established based on the characteristics of the location, where the geometry, soil properties, water levels, and loads are defined. Based on this model, simulations are executed to determine the critical failure state of the dike. Subsequently, various sheet pile designs are evaluated and guided through the incorporation of GrainLearning.

Three different tests were conducted within the machine-learning tool: (1) a variation test to examine the simulation parameters, (2) a location shift test to assess the impact of different positions, and (3) a length reduction test that focuses on reducing the uncertainty associated with the sheet pile length. The results indicate that the optimal sheet pile placement is one meter away from the crest. This design not only satisfies safety but also minimizes sheet pile length. Subsequently, reducing the amount of material required for production, transportation, and construction. This enhances the overall sustainability of a project and ultimately reduces the cost required from man-hours and steel procurement.

# Contents

<b>1</b>	<b>Introduction</b>	<b>3</b>
1.1	Background . . . . .	3
1.2	Problem statement . . . . .	5
1.3	Research gap . . . . .	5
1.4	Study area . . . . .	6
1.5	Research goal and questions . . . . .	6
<b>2</b>	<b>Methodology</b>	<b>7</b>
2.1	Framework . . . . .	7
2.2	PLAXIS . . . . .	8
2.2.1	Soil constitutive model - Mohr-Coulomb (MC) . . . . .	8
2.2.2	Factor of safety . . . . .	9
2.3	Location's characteristics . . . . .	10
2.4	Loading conditions . . . . .	11
2.5	Sheet pile implementation . . . . .	11
2.6	GrainLearning: Theory . . . . .	12
2.6.1	Python . . . . .	14
2.7	GrainLearning: Execution . . . . .	14
2.7.1	Variation tests . . . . .	14
2.7.2	Location shift test . . . . .	15
2.7.3	Length reduction test . . . . .	15
<b>3</b>	<b>Model setup and justification</b>	<b>16</b>
3.1	Location's property . . . . .	16
3.1.1	Mesh influence . . . . .	17
3.1.2	Soil properties . . . . .	17
3.1.3	Water levels . . . . .	19
3.2	Loads . . . . .	19
3.2.1	Gravity . . . . .	19
3.2.2	Ground pressures . . . . .	20
3.2.3	Water pressures . . . . .	21
3.2.4	Top loadings . . . . .	21
3.2.5	D-Stability verification . . . . .	22
3.3	Sheet pile types . . . . .	23
<b>4</b>	<b>Finite element modeling</b>	<b>26</b>
4.1	Simulation phases . . . . .	27
4.2	Initial dike model analysis . . . . .	27
4.3	Critical failure state determination . . . . .	29

4.4	Sheet pile implementation . . . . .	29
4.4.1	Practical considerations . . . . .	31
4.4.2	Evaluation of Z-type sheet piles . . . . .	32
4.5	Analysis of the dike model including sheet pile implementation . . . . .	33
4.6	Initial model used for GrainLearning . . . . .	34
<b>5</b>	<b>Results</b>	<b>35</b>
5.1	Variation tests . . . . .	35
5.1.1	Ranking variation tests . . . . .	37
5.2	Location shift tests . . . . .	38
5.2.1	Ranking location shift tests . . . . .	41
5.3	Length reduction tests . . . . .	41
5.3.1	Ranking length reduction tests . . . . .	44
5.4	Summary . . . . .	44
<b>6</b>	<b>Discussion</b>	<b>45</b>
<b>7</b>	<b>Conclusion</b>	<b>47</b>
<b>8</b>	<b>Recommendations</b>	<b>48</b>

# 1 Introduction

This chapter presents an overview of the context of the Master thesis research by outlining the background, problem statement, research gap, study area research goal, and research questions.

## 1.1 Background

Dikes are an important part of human infrastructure, built to protect the hinterland from flooding induced by natural phenomena such as precipitation, overflow, storms, and rising water levels. These embankments are constructed along rivers, coastlines, canals, and other water surfaces to mitigate inundation risk, protecting human lives and property in regions vulnerable to flooding (Bijker, 2007). In the past 50 years, floods have resulted in significant human deaths, economic losses, and property destruction. Of all natural disasters occurring globally, floods, have been the most frequent phenomena (Douben, 2006). One example is the flood that struck Hat Yai, Thailand, in the year 2000, resulting in at least 32 human deaths, 1700 injuries, and extensive property damage. Additionally, such disasters have negatively affected the mental health of populations (Assanangkornchai et al., 2004).

With continuous climate changes and global warming, the frequency of such events is likely to increase. Heavy rainfall causes overflow within the water surfaces while rising sea levels further worsen the dike's structural integrity. Therefore, it is important to enhance dike sections to ensure the resilience of these structures (Hoekstra and De Kok, 2008).

One method of dike reinforcement involves the usage of sheet piles, which are driven vertically into the embankment to provide additional strength against multiple failure mechanisms. However, installing these sheet piles negatively impacts economic costs and sustainability, which are important considerations in engineering practices (Abd Alghaffar and Dymiotis-Wellington, 2004). The design of resilient flood defenses is an important investment where cost-saving measures could make such hydraulic engineering projects more feasible. Furthermore, sustainable aspects must be integrated into the process to minimize emissions associated with the production, transportation, construction, and maintenance of these structures (Fohl and Hechler, 2023).

Within the context of dike stability, macro-stability failure (slope sliding) considers two zones: the active zone (driving zone) and the passive zone (resistance zone). The active zone consists of the dike structure, while the passive zone contains the hinterland. Achieving equilibrium between the two zones is important, but can be negatively affected by horizontal compression (shear stresses) exerted by the active zone onto the passive zone (STOWA, 2007; Warmink, 2023). The two zones are shown in the figure below.

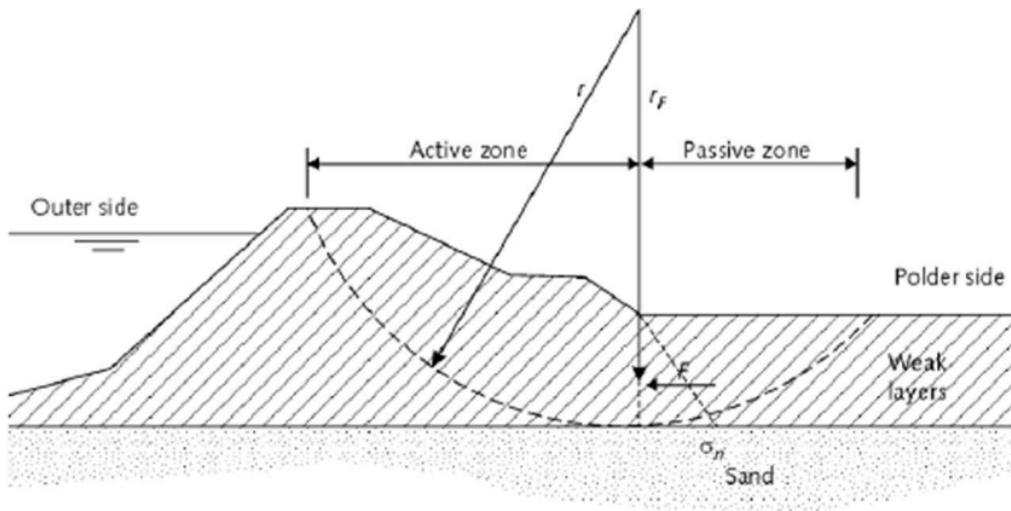


Figure 1: Sketch of macro-stability failure, highlighting the active and passive zone (Warmink, 2023)

Macro-stability can occur in two primary factors:

1. *Increase in water pressure:* An increase in water levels on the waterside of the dike results in increased pressure on the dike. The additional hydrostatic pressure can lead to erosion of soil layers, weakening the dike's integrity. Potentially, leading to a displacement of the active zone into the passive zone, resulting in shear failure;
2. *Drought conditions:* Extended dry periods can lead to desiccation of certain soil layers, such as peat, reducing the weight and strength of the dike. Subsequently, the dike becomes more vulnerable to external water pressures, resulting in potential shear failure (Warmink, 2023).

Macro-stability may occur by fluctuations in water levels on the waterside. During high water states (typically in winter periods), elevated water pressures are exerted upon the dike, allowing for water absorption by certain soil layers (specifically sand). This phenomenon can increase pore pressures and the reduction of effective stress. Potentially, increasing the effect of soil liquefaction and subsequently erosion of the dike, thereby increasing the risk of slope sliding (Visser, 1999).

When transitioning to low-water states (typically in summer periods), the remaining water within the dike maintains the active zone while the waterside becomes the passive zone. If the pressures within the dike exceed a critical threshold, erosion can initiate. Subsequently, slope sliding may occur (Visser, 1999). The implementation of sheet piles strengthens the structure and restores equilibrium between the two zones, thereby reducing the risk of failure (Warmink, 2023).

## **1.2 Problem statement**

In current engineering practice, sheet piles are primarily designed to withstand the driving forces, but the integration of sustainability aspects into their design remains uncommon. The main focus is on engineering performance, with safety being the priority. Incorporating sustainability into the process has the potential to reduce overall emissions and costs.

For the analysis and design, the finite element software PLAXIS is employed, known for its use in geotechnical engineering applications (Exley, 2024). A challenge exists in achieving a balance in the design of sheet piles when including engineering performance, sustainability aspects, and cost-efficiency. Hereby, the length and placement of the piles within the dike are important in achieving an optimized design that meets all these criteria.

Specifically, it is essential to minimize the length of the sheet pile to the greatest extent possible while ensuring that it can withstand the pressures exerted upon the dike. Within PLAXIS, a safety factor is calculated, indicating the safety of the dike model. This safety factor value is dependent on the characteristics of the location, and a minimum design value must be maintained to ensure the dike's safety.

Therefore, the objective of this research is to minimize the length of the sheet pile while attaining a safety factor value that is as close to the design value. Hereby, the goal contributes to sustainable engineering practices for optimized sheet pile designs in dikes by including safety, sustainable aspects, and cost-efficiency.

## **1.3 Research gap**

Sustainability in construction and engineering has been an important aspect in recent years, particularly regarding the reuse of materials. Notably, the reuse of materials can reduce environmental impacts. In the context of sheet pile design within dikes, the placement and length of the piles are important factors that influence the overall impact, due to the consumption of the material (Fohl and Hechler, 2023).

Therefore, the goal is to achieve an optimized design for the sheet pile that integrates engineering performance, sustainability aspects, and cost-efficiency. Hereby, multiple combinations of sheet pile placements and lengths will be tested using PLAXIS. Furthermore, the integration of machine learning, such as GrainLearning, will improve the efficiency of the analysis. This tool utilizes Bayesian calibration and quantifies uncertainties of simulations related to geotechnical engineering (Cheng et al., 2024).

## 1.4 Study area

The eastern region of the Netherlands is characterized by sand dikes along the river IJssel. Slope sliding of these dikes on the waterside is negatively affected by fluctuations in water levels, due to their non-cohesive and permeable property. The permeability allows the water to infiltrate the soil and erosion may occur. This results in a landslide effect along the slope, which is worsened by top loadings from vehicles and machines on the crest (van Hoven et al., 2010).

This research focuses on a specific location: a pumping station located within a dike in the province of Gelderland, in Terwolde (Water in Polder Nijbroek, n.d.).

## 1.5 Research goal and questions

The goal of this research is to investigate and determine the optimal sheet pile design for a sand dike, specifically under critical failure conditions at the pumping station in Terwolde. The goal is formulated in the following main research question:

*What is the optimal sheet pile design for the sand dike structure in critical failure state at the pumping station in Terwolde?*

To achieve the main research question, the following questions will be investigated:

1. How can the sand dike's characteristics in a critical failure state be defined to build a finite element model using PLAXIS?
2. What are the characteristic loading conditions that are present within the area that have to be incorporated into the simulations?
3. What sheet pile designs should be evaluated within the finite element model to ensure a standard design that guarantees the design value?
4. What are the effects of varying lengths and placements of sheet piles on the design of the dike structure utilizing GrainLearning?

## 2 Methodology

This chapter describes the methodology for achieving the goal of the Master's thesis. For each question, the steps and requirements are explained. Additionally, a framework is established to enhance the understanding of the methodology.

### 2.1 Framework

The framework of the Master thesis is shown below. This research requires two primary software tools for the analysis: PLAXIS and GrainLearning. Detailed information on the application of the tools is provided in the paragraphs 2.2, 2.6, and 2.7.

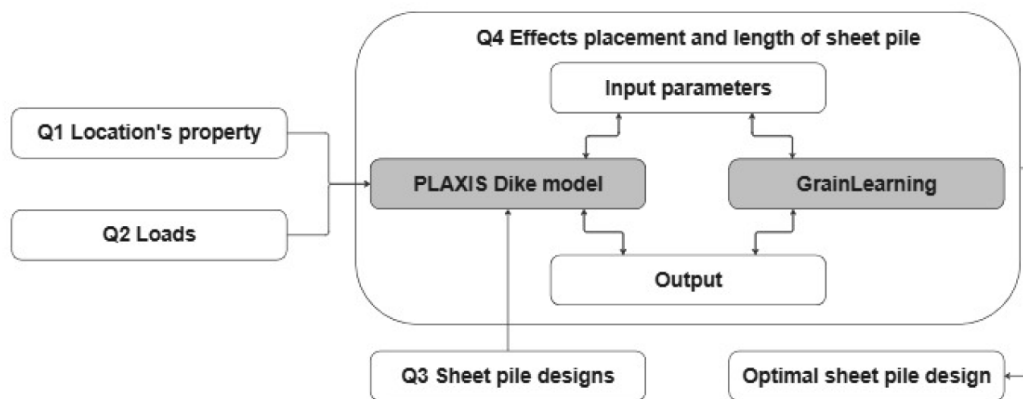


Figure 2: Framework of the methodology for the Master thesis

Initially, the characteristics and loading conditions of the study area will be implemented within PLAXIS. Based on this model, the critical failure state is determined by including water level fluctuations and simulating a potential landslide scenario, leading to dike failure.

Subsequently, various sheet pile designs are assessed under the critical failure state to ensure the design value. The most optimal sheet pile design will then be used as the initial design for further optimization in GrainLearning.

Grainlearning enables the analysis of multiple configurations regarding sheet pile placement and length, derived from the initial design. New input will be generated, allowing for re-implementation into PLAXIS. This iterative process ensures new output including updated safety factors. The output will be used back into GrainLearning to refine the input and improve the sheet pile design.

Through the iterative process between the two software tools, various sheet pile configurations are thoroughly analyzed. The sheet pile configurations will be assessed to determine the optimal design.

## 2.2 PLAXIS

In geotechnical engineering, finite element models (FEM) are used regularly in analyzing the stability of structures. The structure is separated into multiple interconnected elements, and the internal state of the structure is calculated via numerical methods. This approach allows the software to generate a comprehensive representation of the interconnected elements, describing the behavior of the model. The output of the FEM provides insight into the deformations, strains, and safety of the model, which would be time-consuming and expensive if executed through real-life experiments (van Adrichem, 2021; Delft University of Technology, 2016).

Furthermore, it is essential to include the established guidelines in the research to obtain a representative model. Specifically, the guidelines CUR 166 and NEN 9997 provide information on sheet pile application and FEM design process. These guidelines ensure that the analysis is executed systematically and reflects practical considerations (CUR, 2023; NEN, 2017).

### 2.2.1 Soil constitutive model - Mohr-Coulomb (MC)

The selection of a suitable soil constitutive model is important to determine the behavior of soil layers. For this research, the Mohr-Coulomb model is chosen, which is elaborated in paragraph 3.1.2. Below, is a description of the Mohr-Coulomb model.

The Mohr-Coulomb model describes the linear elastic perfectly-plastic behavior of the soil (see figure 3). This model allows initial analysis results derived through first-order calculations. Assuming a constant stiffness per layer, which increases linearly in depth. Ensuring a rapid approach for simulating soil mechanics (PLAXIS, 2015).

Failure within the model occurs when the stress reaches the strength of the soil, which is expressed in terms of principal stresses. The belonging equation is shown below (Maatkamp, 2016).

$$\sigma_1 = \frac{2c \cos \phi - 2\sigma_3 \sin \phi}{1 - \sin \phi} \quad (1)$$

Where the parameters are defined as:

1.  $\sigma_1$ , major principal stress;
2.  $\sigma_3$ , minor principal stress;
3.  $c$ , cohesion;
4.  $\phi$ , friction angle;

Regarding plastic behavior, the development of the strains are unable to revert to their original form after yielding. Hereby, a yield function is employed that indicates the border between

the elastic and plastic domains of the soil material. In the elastic domain, the soil behaves according to Hooke's law, and the strain can revert to its original form. Upon reaching the border, the soil fails, resulting in permanent deformation. The elastic domain ( $\epsilon^e$ ) and plastic domain ( $\epsilon^p$ ) are shown in the figure below (PLAXIS, 2015).

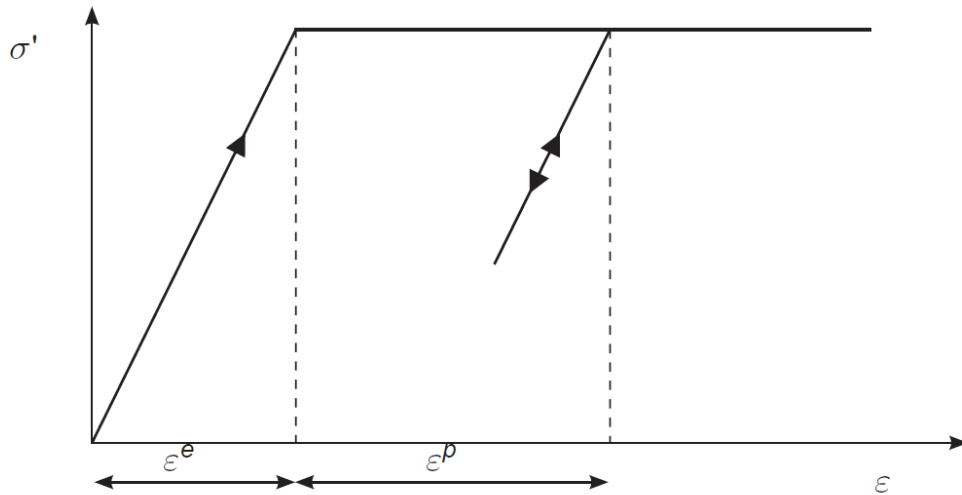


Figure 3: Illustration of the elastic perfectly-plastic model (PLAXIS, 2015)

For the calculations in PLAXIS, the parameters below are required (Levasseur et al., 2008; Yin et al., 2018).

1. Elasticity modulus ( $E$ ), deformation under stress;
2. Friction angle ( $\phi$ ), the angle due to internal friction;
3. Dilatancy angle ( $\Psi$ ), volume change under shear stress;
4. Cohesion ( $c$ ), measure level of adhesion between soil particles;
5. Poisson ratio ( $\nu$ ), ratio level between lateral and axial strain.

The Mohr-Coulomb model forms the foundation for modeling soil properties as it accommodates shear strength parameters and is rapidly implemented within PLAXIS (Levasseur et al., 2008; Yin et al., 2018). Additionally, when implementing interface elements such as sheet piles, the system selectively uses relevant parameters (PLAXIS, 2015).

### 2.2.2 Factor of safety

The determination of the stability of the dike model requires a factor of safety calculation. This involves establishing the design value that the model must maintain to ensure structural integrity. Therefore, the phi/c reduction method (Bentley, 2023) is employed within PLAXIS to determine the safety factor value. The parameters friction angle ( $\phi$ ) and cohesion ( $c$ ) are reduced until the model reaches the failure state, and are expressed in the equation below (Arinze and Okafor, 2017).

$$RF = \frac{\tan \phi_i}{\tan \phi_r} = \frac{c_i}{c_r} \quad (2)$$

Hereby, the parameters are:

1.  $RF$ , reduction factor;
2.  $\phi_i$ , friction angle input value;
3.  $c_i$ , cohesion input value;
4.  $\phi_r$ , reduced friction angle value;
5.  $c_r$ , reduced cohesion value.

### 2.3 Location's characteristics

In the context of PLAXIS modeling, it is important to develop a model that incorporates the characteristics of the location, including the geometry, soil properties, mesh grid, and water levels.

The geometry is derived from the Dutch Elevation model: Actueel Hoogtebestand Nederland (AHN), where elevation is referred to Normaal Amsterdams Peil (NAP) (AHN, 2024). The geometry of the dike model is modified to reflect the critical failure state, which is the condition where the safety factor is below the design value. This analysis includes the erosion and sliding effect on the slope that affect the overall stability of the dike.

Soil properties and water levels are determined from the technical report associated with the pumping station in Terwolde (Sasse, 2023). The mesh grid generation is based on a medium grid to ensure a balance between computational time and result accuracy (Liu, 2013).

The parameters of the Mohr-Coulomb model mentioned in paragraph 2.2.1, with a range of additional parameters will be used to obtain accurate results of the model. These parameters are shown below and are determined via literature, the guidelines, and the technical report (Exley, 2024; Kahlström, 2013; NEN, 2017; Sasse, 2023).

Parameter	Description	Abbreviation	Unit
Drainage type	Material behavior regarding pore pressure and permeability	-	-
Dry unit weight	The unit weight of the material when it is dry	$\gamma_{unsat}$	kN/m <sup>3</sup>
Saturated unit weight	The unit weight of the material when it is wet	$\gamma_{sat}$	kN/m <sup>3</sup>
Initial void ratio	Ratio of voids against the solid particles in a soil layer	$e_0$	-
Initial porosity	Ratio of voids against the total volume in a soil layer	$n_{init}$	-
Young's modulus	Deformation under stress	E	kN/m <sup>2</sup>
Poisson ratio	Ratio level between lateral and axial strain	$\nu$	-
Cohesion	Measure level of adhesion between soil particles	c	kN/m <sup>2</sup>
Friction angle	The angle due to internal friction	$\phi$	°
Dilatancy angle	Volume change under shear	$\Psi$	°
Horizontal permeability	Measure of water that can pass through the soil horizontally	$k_x$	m/day
Vertical permeability	Measure of water that can pass through the soil vertically	$k_y$	m/day
Cross permeability	Level of permeability of the soil	-	-
Hydraulic resistance	How much water can get through the soil	d/k	day
Drainage conductivity	Total amount of water that is transported through the pores	dk	m <sup>3</sup> /day/m

Table 1: Soil parameters utilized in the PLAXIS model

## 2.4 Loading conditions

The application of loading conditions is important within the FEM to assess the dike's stability under several forces which it has to resist (Bree van et al., 2011). The specific values and applications on the dike are derived from the NEN guideline 9997 (NEN, 2017). Constraints and location characteristics are incorporated to ensure realistic estimations for the loading conditions.

Furthermore, simulation phases are established for loads that exhibit temporal variability. This approach assesses the dike in different circumstances and tests its resilience. The initial phases consist of simulations where different water levels are applied to the dike to obtain the model's equilibrium. Subsequently, the sheet pile is implemented within the model, including top loadings from vehicles and machines. This scenario is simulated for the different water level states to ensure the structural integrity of the dike. Finalized by simulations in the critical failure state of the dike, also in combination with different water level conditions.

## 2.5 Sheet pile implementation

Assessing the interaction between soil and structural components within the FEM requires interface element modeling (IEM). This ensures the examination of various sheet pile designs within the model, providing insights into the soil-structure behavior such as deformation and stresses.

The design of sheet piles requires information from the guideline CUR 166 and the literature review (CUR, 2023). Key material parameters are required for the simulation of the model, which are described below (Pantev and Rutgers, 2022; PLAXIS, 2015).

1. Weight ( $w$ ), the mass of the pile;
2. Axial stiffness ( $EA_1$ ), Young's Modulus ( $E$ ) times the cross-sectional area ( $A$ );
3. Stiffness in the out-of-plane direction ( $EA_2$ ), Young's Modulus ( $E$ ) times the second cross-sectional area ( $A$ );
4. Bending stiffness ( $EI$ ), the Young's Modulus ( $E$ ) times the second moment of inertia ( $I$ );
5. Poisson ratio, the ratio between lateral and axial strain. Typically 0.33 for steel (Greaves et al., 2011).

PLAXIS 2D calculations employ the X and Y coordinates, and the width is only included in 3D simulations (Z-coordinate) to execute a trajectory of a dike. The cross-section of a PLAXIS 2D simulation has a standard width of one meter, thus, the implementation of a standard sheet pile design has to be scaled to this measurement (Bentley, 2023). Regarding the calculation of the sheet pile parameters, including the scaled measurement, a standardized Young's modulus value of  $240 \text{ N/mm}^2$  is used (Yamaguchi et al., 1998).

Sheet pile application within civil engineering requires analysis to ensure the engineering performance under several loading conditions. Various structural designs can impact structural integrity and sustainability. Executing a sensitivity analysis on different sheet pile types can enhance the selection of a pile type. This involves the identification of common lengths and placements. Subsequently, a specific design can then be facilitated with the help of GrainLearning, but its parameters are not considered for optimization.

## 2.6 GrainLearning: Theory

The parameters for optimization are the location and length of the sheet pile, identified as variables X and Y within PLAXIS. Executing sensitivity analysis, wherein various positions and lengths are tested, is time-consuming. The integration of GrainLearning provides a more efficient process, whereby the selection process is automated.

The GrainLearning tool exploits the Bayesian inference method, which allows the inference of input based on system outputs. In this approach, the Bayes theorem is applied and shown below (Cheng et al., 2024).

$$p(A|B) = \frac{p(B|A)p(A)}{p(B)} \quad (3)$$

The parameters are defined as follows:

1.  $p(A|B)$ , probability of A given that B has occurred (posterior);
2.  $p(B|A)$ , probability of B given that A has occurred (likelihood);
3.  $p(A)$ , probability of A (prior);
4.  $p(B)$ , probability of B, which is a constant that ensures the distributions to be a total sum of one (normalizing factor).

Hypothesis A represents the input: the length of the sheet pile. Hypothesis B consists of the model output: the safety factor value. GrainLearning attempts to infer optimal values for the input by combining the two hypotheses into probabilities:

1. Probability of the input;
2. Probability of a certain output based on a certain input.

The computation requires the multiplication of these probabilities to obtain a measure that reflects the coherence between the input and output. This iterative process is executed continuously with varying inputs to identify the best configuration.

The output of GrainLearning consists of probability distributions of the posterior, likelihood, and prior, and are evaluated through sampling. Weights are assigned to the samples, reflecting the probabilities (see figure below) (Cheng et al., 2024).

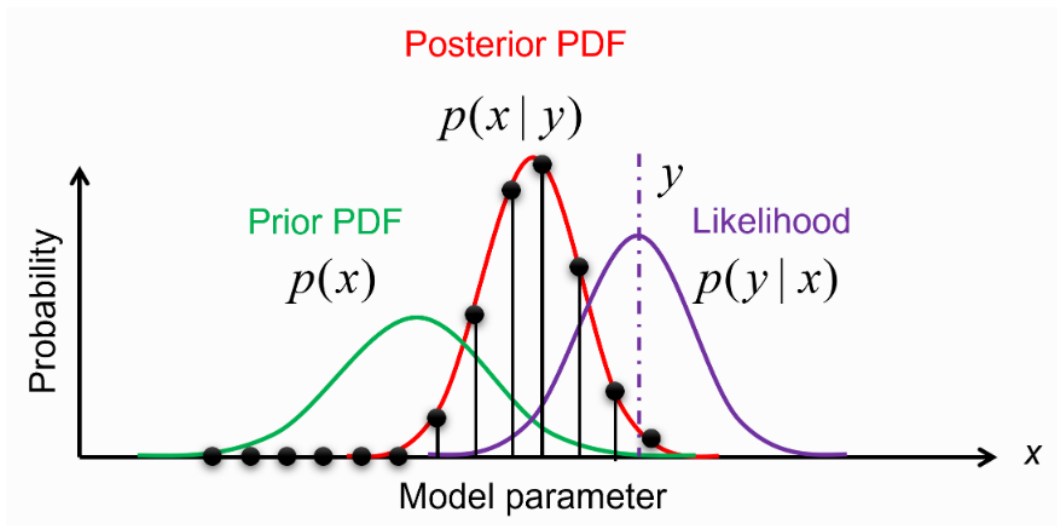


Figure 4: Distributions for the prior, posterior, and likelihood derived from the Bayesian inference (Cheng et al., 2024)

The three distributions describe the following:

1. Prior, the probability density function of the model input;
2. Likelihood, how likely the output matches the input;
3. Posterior, probability density function of the likelihood between combinations of input based on the output.

After establishing the distributions, GrainLearning identifies the most probable combination of input based on observed output.

The procedural steps in GrainLearning are as follows:

1. Generation of initial samples within a specific range for the input;
2. Execution of the Bayesian model;
3. Generation of new distributions;
4. Generation of new samples derived from the updated distributions, followed by reiteration of the procedure.

This iterative process ensures the determination of the most optimal combination of input, corresponding to the output (Cheng et al., 2024; Linnemann, 2024).

### 2.6.1 Python

The primary objective of the integration between GrainLearning and PLAXIS is to ensure that the simulations align closely with the predefined design value. The integration requires the development of a Python script for managing the input and output effectively. Specifically, the script must include the modification of input that corresponds to sheet pile designs. Thereby, the output must yield the safety factor values from the simulations.

## 2.7 GrainLearning: Execution

The top coordinates of the sheet pile remain constant, while the Y-coordinate of the bottom point is varied during the simulations. The number of iterations, samples, and the minimum and maximum range for the sheet pile depth have to be predefined based on the critical failure state. Regarding the GrainLearning framework, the following setup is employed:

1. The sampling method that is used is the Halton sequence;
2. The standard deviation tolerance is set at 0.1;
3. The determination of the probability distribution is based on the Gaussian function if achievable.

Different types of tests are conducted which are explained below.

### 2.7.1 Variation tests

Variation tests are executed using different numbers of iterations and samples to analyze the effects of various parameters on the optimization of the sheet pile design. The table below indicates the specific parameters employed in the variation tests, with the default parameters highlighted with an underline.

Parameter	Values			
Iterations	3	<u>5</u>	8	8
Total number of samples	6	<u>8</u>	8	10

Table 2: Parameter values for the variation tests

The sample count is kept low to mitigate simulation time and enhance the feasibility of this research, acknowledging that this may not retrieve a distribution line for the posterior.

### **2.7.2 Location shift test**

The optimization of the sheet pile design requires testing at different locations to potentially improve safety while minimizing the length. The selection of the locations will be determined after the initial implementation of the sheet pile within the dike in the critical failure state.

Reducing the length of the sheet pile can be executed simultaneously with this test. However, to ensure that the model is not able to skip certain locations and to minimize the computational time, this is executed separately.

### **2.7.3 Length reduction test**

After the simulations from the variation tests and location shift tests, the most probable value identified through GrainLearning will be implemented within PLAXIS. This process facilitates the evaluation of the model's capability to achieve the design value. Should the results indicate a verified value, alternative ranges of parameters will be explored to further reduce the sheet pile length. Should the results indicate an invalid safety factor value, the range has to be extended.

### **3 Model setup and justification**

This chapter addresses the first three questions by describing the characteristics of the location, loading conditions, and sheet pile designs. A standard dike model is set up for the interaction between PLAXIS and GrainLearning. However, the integrity of this model must be validated through comparative studies, existing literature, and alternative modeling software, specifically D-Stability.

Initially, the modeling choices are investigated through literature and studies. This includes aspects such as geometry, mesh grid, and the selection of the soil constitutive model. Mohr-Coulomb is employed due to the applicability of the location's characteristics, and its advantages are explained in detail within paragraph 3.1.2. Subsequently, the loading conditions are set up according to the established guidelines. This procedure ensures a realistic model that aligns with current engineering practices. Following with the identification of a suitable sheet pile type for the dike model.

#### **3.1 Location's property**

The geometry of the dike model is shown in figure 5. The dike exhibits a width of 100 meters, with a maximum depth of -15 meters NAP. The crest of the dike is established at 8.7 meters NAP, with a width of 20 meters. The slopes extend on both sides of the dike, each gradually descending over a distance of 10 meters.

A similar study executed in Karolinka, Czech Republic, demonstrated a comparable dike geometry for the slope stability assessment and potential sliding failures using PLAXIS software. A dam was modeled to strengthen the dike its resilience against slope sliding (Bredy and Jandora, 2019).

Additionally, research by the Delft University of Technology regarding the implementation of tailings dams has proven that outward slope sliding can similarly be analyzed in PLAXIS, utilizing similar geometric configurations (Laera et al., 2024).

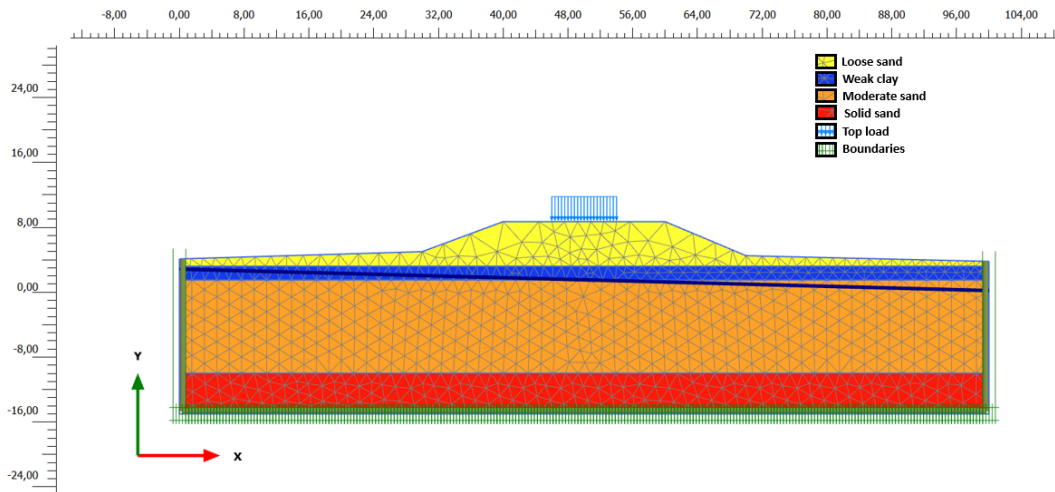


Figure 5: Dike model in PLAXIS of the pumping station in Terwolde

### 3.1.1 Mesh influence

A normal grid is employed for the mesh generation to balance the computational time and result accuracy. This grid configuration can analyze varied changes in stresses and deformations along the slope as described in the research by the Delft University of Technology (Laera et al., 2024). Additionally, a complementary study from the same institute indicates that mesh refinement does not automatically reduce the safety factor with a comparable geometry (van Adrichem, 2021).

### 3.1.2 Soil properties

Four different soil types are identified and incorporated into the model, as illustrated in figure 5. Yellow corresponds to loose sand, while blue represents weak clay. Moderate sand is depicted by the orange layer, and the red layer represents solid sand. The soil layers are present in varying depths and their parameter values are described in the table below (Kahlström, 2013; NEN, 2017).

<i>Parameter / Soil type</i>	<b>Sand, loose</b>	<b>Clay, weak</b>	<b>Sand, moderate</b>	<b>Sand, solid</b>
<b>Upper layer [m NAP]</b>	+8.70	+3.20	+1.50	-10.00
<b>Bottom layer [m NAP]</b>	+3.20	+1.50	-10.00	-15.00
<b>Drainage type</b>	Drained	Undrained A	Drained	Drained
$\gamma_{unsat}$ [kN/m <sup>3</sup> ]	17	14	18	19
$\gamma_{sat}$ [kN/m <sup>3</sup> ]	19	14	20	21
$e_0$	0.65	0.80	0.45	0.35
$n_{init}$	0.39	0.44	0.31	0.26
<b>E [kN/m<sup>2</sup>]</b>	25000	10000	45000	75000
$\nu$	0.35	0.40	0.25	0.15
<b>c [kN/m<sup>2</sup>]</b>	0	0	0	0
$\varphi$ [degrees]	30	17.5	32.5	35
$\Psi$ [degrees]	0	0	2	5
<b>k<sub>x</sub> [m/day]</b>	1e-4	1e-9	1e-5	1e-4
<b>k<sub>y</sub> [m/day]</b>	1e-4	1e-9	1e-5	1e-4
<b>Cross permeability</b>	Semi	Impermeable	Semi	Fully
<b>Hydraulic resistance [day]</b>	1e-6	-	1e-5	-
<b>Drainage conductivity [m<sup>3</sup>/day/m]</b>	1.0	0	5	1e-4

Table 3: Soil parameters used within the model for each soil type (Kahlström, 2013; NEN, 2017)

The Mohr-Coulomb model is an appropriate model for implementing interface elements such as sheet piles. This model effectively incorporates relevant parameters, minimizing potential unrealistic shear deformation values during the analysis. Furthermore, the homogeneous sand layers within the dike, enable the Mohr-Coulomb failure criterion to be applied effectively (PLAXIS, 2015).

Prior research demonstrated the application of Mohr-Coulomb for sand models obtaining reliable results in PLAXIS. The study executed by Delft University on the implementation of a dam is one example, where the macro-stability failure was analyzed (Laera et al., 2024). Another study on dike stability has revealed that the Mohr-Coulomb and Hardening Soil models produce comparable results in terms of the safety factor values (Tu and van Gelder, 2013).

The application of sheet piles in dikes has been previously investigated, with findings indicating that the implementation of the Mohr-Coulomb model results in reliable soil-structure interactions (Rippi et al., 2016).

### 3.1.3 Water levels

The assessment of slope stability requires the implementation of seasonal variations in water levels. For this study area two seasonal water levels are employed, corresponding to the winter and summer periods. Specifically, for both periods the low and high water levels within the river and hinterland are used and shown below (Sasse, 2023).

1. Mean high water level MHWL in hinterland = 3.5 m;
2. Mean high water level MHWL in river = 7.1 m;
3. Mean low water level MLWL in hinterland = 2.85 m;
4. Mean low water level MLWL in river = 0.20 m.

Previous studies have proven that variations in water levels significantly influence slope stability. Higher water levels tend to increase the vulnerability of dikes. However, this is dependent on the values of the soil properties. Specifically, the (un)drained state of the soil (Pham et al., 2024).

## 3.2 Loads

The design of geotechnical structures is according to the guideline NEN 9997 in practice engineering. In this research, the focus is on the macro-stability failure, only loads that influence the failure mechanism are considered, as shown below (NEN, 2017).

Load	Unit	Value	Remarks
Weight of the soil and water	m/s <sup>2</sup>	9.81	Gravity
Ground pressures			Dependent on the soil materials
Water pressures			Dependent on the water levels
Groundwater pressures			Dependent on the water levels
Top loadings	kN/m <sup>2</sup>	20	Machines and traffic

Table 4: Loads used in PLAXIS

The loads impacting the dike, include gravitational, ground, water, and surface pressures. Other loading conditions are investigated but concluded to have minimal influence on the dike structure.

### 3.2.1 Gravity

The gravity is a constant value of  $g = 9.81 \text{ m/s}^2$  (Terzaghi, 1943). Combined with the weight of the soil and the water, the calculation of the vertical self-weight stress of the dike structure is presented. This stress is linearly proportional to the depth within a homogeneous soil, and its stress distribution is shown below (Yu, 2023).

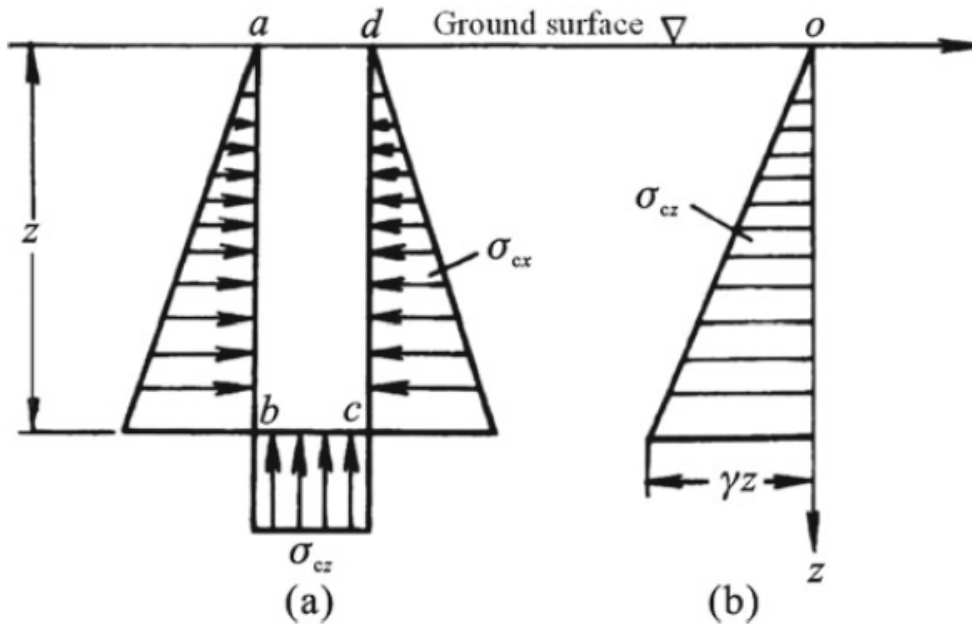


Figure 6: Homogeneous soil vertical stress distribution (Yu, 2023)

This stress distribution is influenced by the soil moisture content. Variations in stress results are due to differences in soil properties. For the calculation of the stress, the density of the soil ( $\gamma$ ), and the depth ( $z$ ) are multiplied by each other (Yu, 2023):

$$\sigma = \gamma * z \quad (4)$$

### 3.2.2 Ground pressures

Ground pressures are influenced by the soil material properties, as described in paragraph 3.1.2 (Exley, 2024). To comprehend the behavior of the soil, fundamental principles and equations are established, and described below (PLAXIS, 2015; Terzaghi, 1943).

#### Normal and shear stress

Stress is defined as the force per unit area. A distinction exists between the normal stress ( $\sigma$ ) and shear stress ( $\tau$ ). Normal stress is the perpendicular stress on a surface, while shear stress is the parallel stress acting along the surface (Macciotta, 2018).

#### Effective stress

The effective stress ( $\bar{\sigma}$ ) is defined as the total stress ( $\sigma$ ) without the water pore pressure ( $u$ ), as shown in the equation below. This stress is important for assessing the compaction, strength, and deformation of the soil (Terzaghi, 1943).

$$\bar{\sigma} = \sigma - u \quad (5)$$

### **Stress-strain relationship**

The strain ( $\epsilon$ ) represents the deformation that occurs in response to the applied stress ( $\sigma$ ). This relationship is characterized by Young's modulus of the soil ( $E$ ) and predicts the soil behavior under various loading conditions. For this research, the Mohr-Coulomb model is based on Hooke's law (Bobrowsky and Marker, 2018):

$$\epsilon = \frac{\sigma}{E} \quad (6)$$

### **3.2.3 Water pressures**

The analysis of water pressures consists of the surface water and groundwater pressures and is processed in two seasonal stages. Each season represents a half year to assess the soil behavior. The response is dependent on the drainage type of the soil material. Drained conditions allow the dissipation of water, while undrained conditions lack this ability due to a lower permeability of the soil (PLAXIS, 2015).

### **3.2.4 Top loadings**

The traffic loadings are important in evaluating the dike's stability. According to the guidelines, the maximum allowed traffic loading is established at 50 tonnes, which almost equals  $500 \text{ kN/m}^2$ , considering the gravitational acceleration ( $50 \cdot 9.81$ ) (CUR, 2023). This load is distributed over the roadway's width, which equals 3.5 meters on each side and is further divided by the front and back axis for each wheel. This results in a loading of  $35.71 \text{ kN/m}^2$  ( $500 \text{ kN/m}^2 / 3.5 \text{ m} / 4 \text{ wheels}$ ). However, such loading conditions are rarely present in the study area. Considering the typical traffic loadings and construction machines for the installation of sheet piles, a more realistic loading of  $20 \text{ kN/m}^2$  is determined (Pantev and Rutgers, 2022).

### 3.2.5 D-Stability verification

All parameters described in previous paragraphs are implemented within the D-Stability software to assess potential sliding effects on the dike model. However, an important note is that not all parameters are integrable due to constraints within the software. Consequently, a replication of the dike model is realized to the fullest extent possible. The outputs and behavior are illustrated in the figures below.

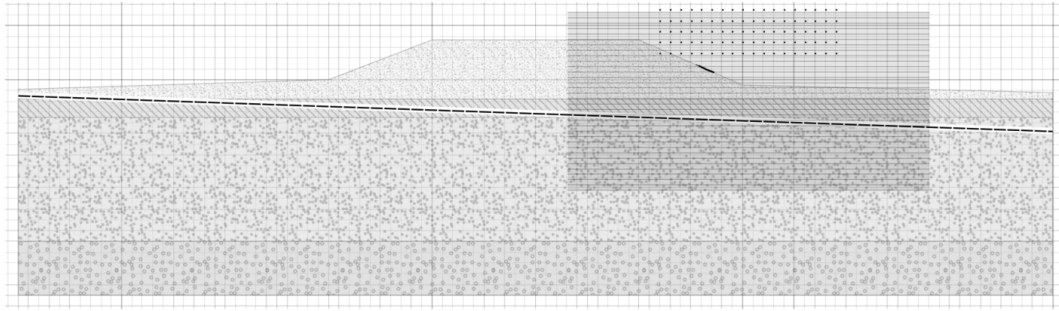


Figure 7: Initial dike model in D-Stability in low water state (FS = 1.197)

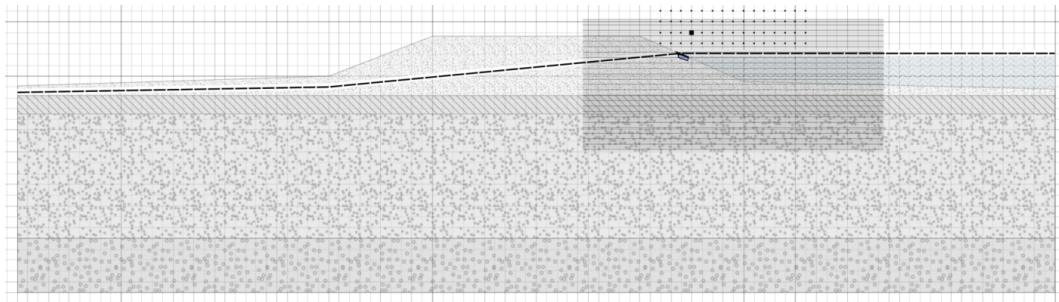


Figure 8: Initial dike model in D-Stability in high water state (FS = 1.117)

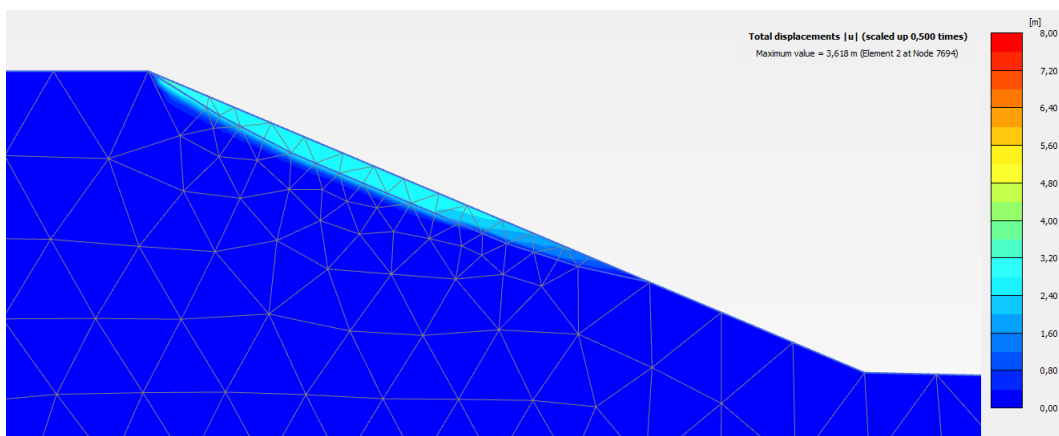


Figure 9: Initial dike model along the slope in PLAXIS in low water state (FS = 1.306)

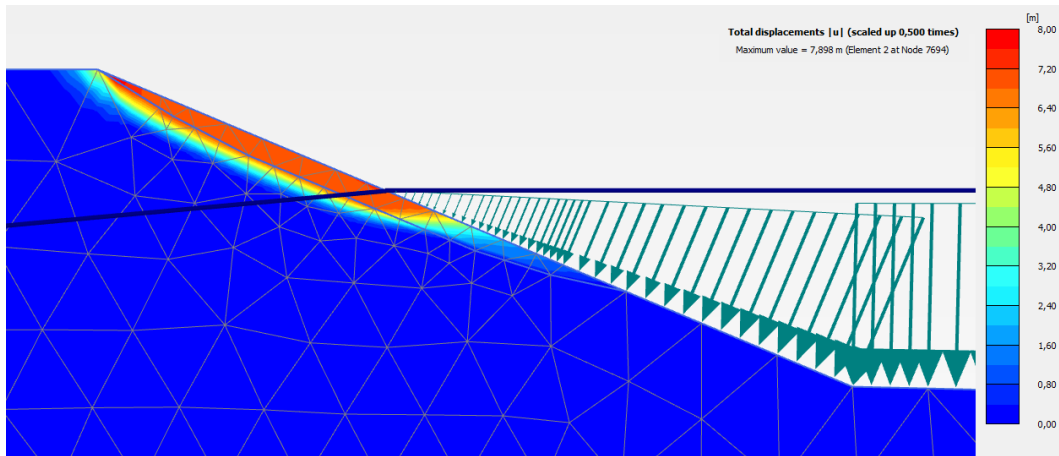


Figure 10: Initial dike model in D-Stability in high water state (FS = 1.286)

Figure 7 indicates the dike in low water conditions, including a safety factor value of 1.197. Figure 8 represents the high water state, including a safety factor value of 1.117. Both scenarios indicate the landslide effect on the outer slope, located at the line of the high water level (Van et al., 2022; Van Hoven et al., 2014).

The landslide effect is also shown in the PLAXIS output for both scenarios (figures 9 and 10). However, the effect occurs more along the top of the slope until the water level and the safety factors are higher. This effect is elaborated in paragraph 4.3 for the determination of the critical failure state.

### 3.3 Sheet pile types

The implementation of sheet piles in civil engineering requires the investigation of multiple sheet pile types. According to the important sheet pile manufacturers, Nanjing Grand Steel Piling Co., Ltd., and ArcelorMittal, three common types are utilized in dike construction to ensure structural integrity (ArcelorMittal, 2024; Nanjing Grand Steel Piling Co.,Ltd, 2024).

#### Z-profile

Z-profile sheet piles are characterized by an interlocking system, wherein one hook is positioned higher than the other. This design allows the attachment of continuous sheet piles at reversed orientation, forming a wall structure as shown in figure 11. The symmetric interlocking mechanism ensures the material's strength. Increasing the width of these piles results in a reduction in the number of piles required, enhancing the water-tightness and reducing the costs of the construction (Nanjing Grand Steel Piling Co.,Ltd, 2024).

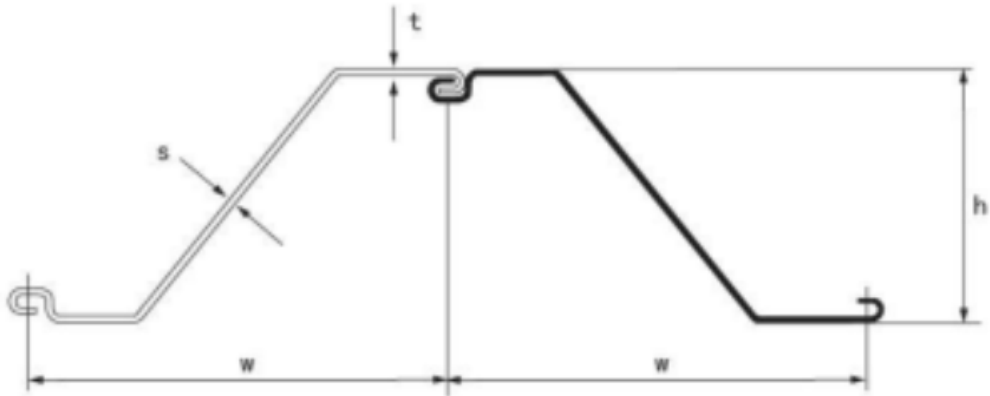


Figure 11: Z-profile sheet pile (Nanjing Grand Steel Piling Co.,Ltd, 2024)

### U-profile

U-profile sheet piles exhibit an interlocking system on both edges, resembling a fusion of two Z-profile sheet piles (see figure 12). This configuration provides a greater moment of inertia per unit compared with the Z-profile. However, Z-profile has been demonstrated to achieve greater strength while maintaining a reduced weight per square meter (Nanjing Grand Steel Piling Co.,Ltd, 2024).

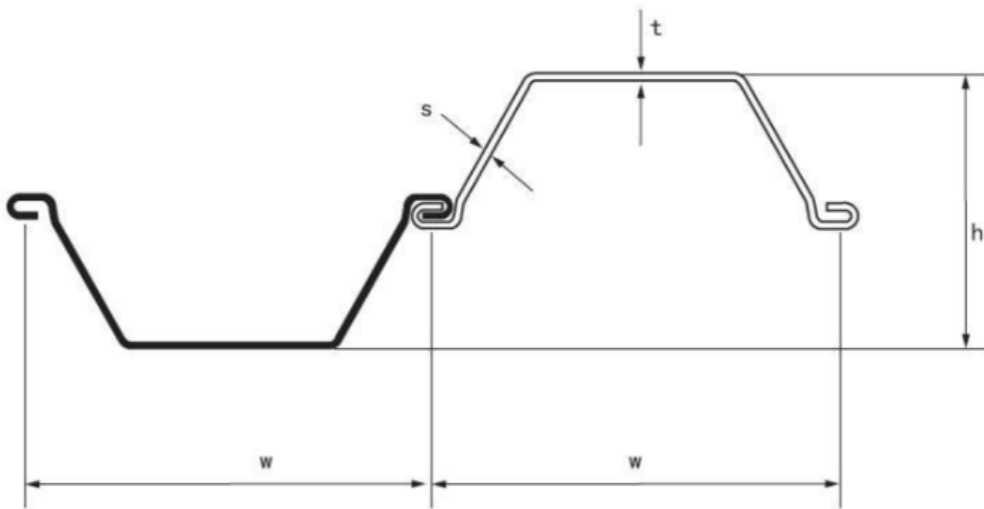


Figure 12: U-profile sheet pile (Nanjing Grand Steel Piling Co.,Ltd, 2024)

### Combi-walls

Combi-wall applications enhance a greater moment in comparison with the Z- and U-profile. This design consists of circular piles 13a) or H-piles (figure 13b), which are interconnected with Z- or U-profile sheet piles 13). However, the implementation of this type inherently costs more due to the increased amount of steel required for production (ArcelorMittal, 2024).

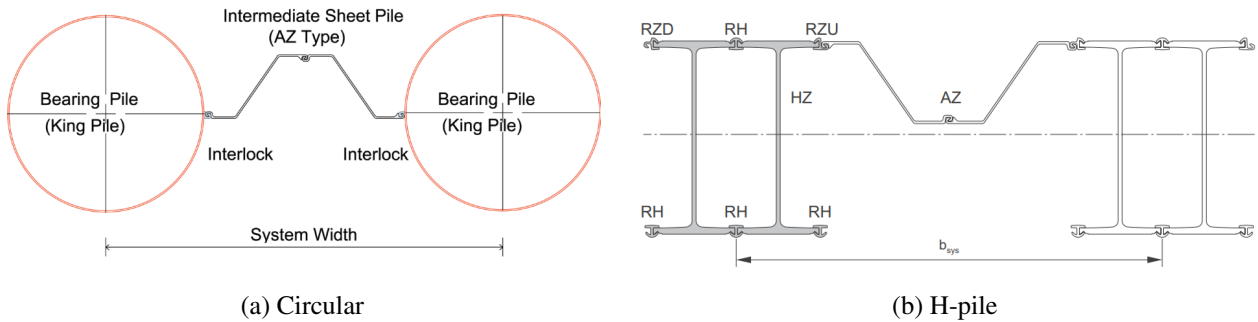


Figure 13: Combi wall sheet pile (ArcelorMittal, 2024)

### Selection sheet pile

Based on the structural advantages and cost considerations of the outlined sheet pile types, the Z-profile is considered the best type and most widely utilized in dike construction. This design can achieve a high resistance against slope sliding, enhancing the structural integrity, and proving to be more economically beneficial. Various configurations of the Z-profile will be investigated in PLAXIS, according to CUR 166 guideline (CUR, 2023).

## 4 Finite element modeling

The finite element model of the dike is developed according to the guideline CUR 166, specifically the design approach OB3. This model incorporates the location's characteristics, loading conditions, and sheet pile design. The steps shown below are important to ensure a reliable model including engineering and modeling considerations (CUR, 2023).

1. Determination of the normative principles;
2. Determination of the characteristic values of the parameters;
3. Determination of the calculation values of the parameters;
4. Selection of the calculation schema between A or B;
5. Calculation of the minimum embedded depth of the pile;
6. Dimensions calculations;
7. Control on the moments;
8. Control on the shear- and normal stresses;
9. Control on the deformations;
10. Taking into account practical aspects.

The initial four steps have been addressed in the previous paragraph 3 and are implemented within PLAXIS. Regarding the calculation schema, schema B has been selected as it assesses the location's characteristics, ensuring a more realistic determination of the applied forces compared to schema A. Furthermore, schema B employs the phi/c reduction method for the calculation of the safety factor (CUR, 2023).

To ensure the dike's safety, the factor of safety has to be determined which is derived from the equation below (Narvaez, 2020).

$$\frac{F}{\gamma_n * \gamma_d * \gamma_s} \geq 1.0 \quad (7)$$

Hereby, the parameters are:

1. Damage factor  $\gamma_n = 1.0$  reflecting the conditions of the location;
2. Model factor  $\gamma_d = 1.0$  due to the application of Mohr-Coulomb;
3. Schematization factor  $\gamma_s = 1.0$  based on the design configurations for the model, supported by guidelines and reports in paragraph 3.

Based on the parameter values, the calculated factor of safety equals 1. Notably, this is the minimum acceptable value for the dike's safety. A safety factor below indicates the dike in its critical failure state.

## 4.1 Simulation phases

The simulation phases have been established based on the timing of the seasonal events, as shown in the table below (Pantev and Rutgers, 2022; van Dongen, 2023)

<i>Phases</i>	<i>Description</i>	<i>Time [days]</i>
<b>Initial</b>	K0 procedure, followed up by two plastic deformation calculations for equilibrium	
<b>Def. LWL</b>	Plastic deformation calculation in low water state	182.5
<b>FS - LWL</b>	Safety factor calculation of previous phase	
<b>Def - HWL</b>	Plastic deformation calculation in high water state	182.5
<b>FS - HWL</b>	Safety factor calculation of previous phase	
<b>Sheet pile installation</b>	Installation of the sheet pile in low water state	30
<b>Top load - LWL</b>	Including top load in low water state	182.5
<b>FS - TL LWL</b>	Safety factor calculation of previous phase	
<b>Top load - HWL</b>	Including top load in high water state	182.5
<b>FS - TL HWL</b>	Safety factor calculation in high water state	
<b>Erosion - LWL</b>	critical failure state of model in low water state	182.5
<b>FS - E LWL</b>	Safety factor calculation of previous phase	
<b>Erosion - HWL</b>	critical failure state of model in high water state	182.5
<b>FS - E HWL</b>	Safety factor calculation of previous phase	

Table 5: Simulation phases

Before the implementation of any sheet pile, the dike must achieve an equilibrium state by processing the initial stresses and deformations. The K0 procedure is employed for the initial state, which includes the vertical stresses of the overlying soil mass. Furthermore, the low- and high-water states are processed to ensure equilibrium, including the plastic deformations in the model. Potential erosion or sliding effects in both states can then be analyzed to determine the critical failure state.

Subsequently, sheet piles are installed, which requires 30 construction days (Pantev and Rutgers, 2022). The top load is then applied during the states, which should be considered for a longer term. Potential erosion or sliding effects determined from the equilibrium state, are then processed in the model to ensure the dike's safety with the implementation of the sheet pile in this critical failure state (van Dongen, 2023).

## 4.2 Initial dike model analysis

The initial dike model involves the dike according to the location's characteristics as described in paragraph 3 without the sheet pile implementation. This approach allows the assessment of the stresses and displacements in its initial equilibrium state and the determination of the dike's behavior. The results for low- and high-water states are shown below.

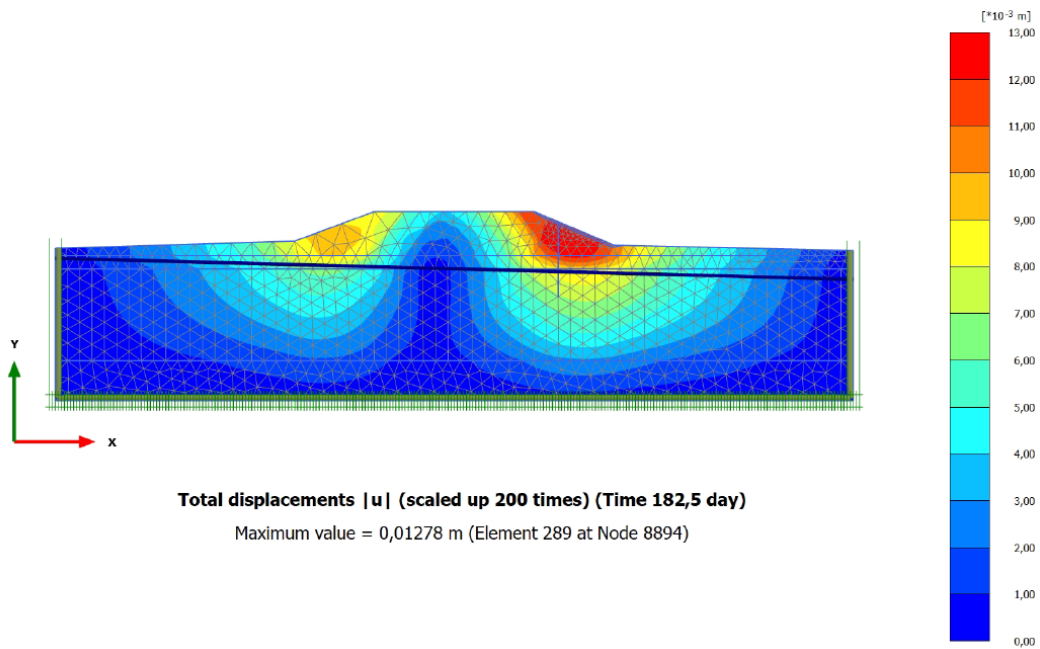


Figure 14: Initial dike model displacements in low water state

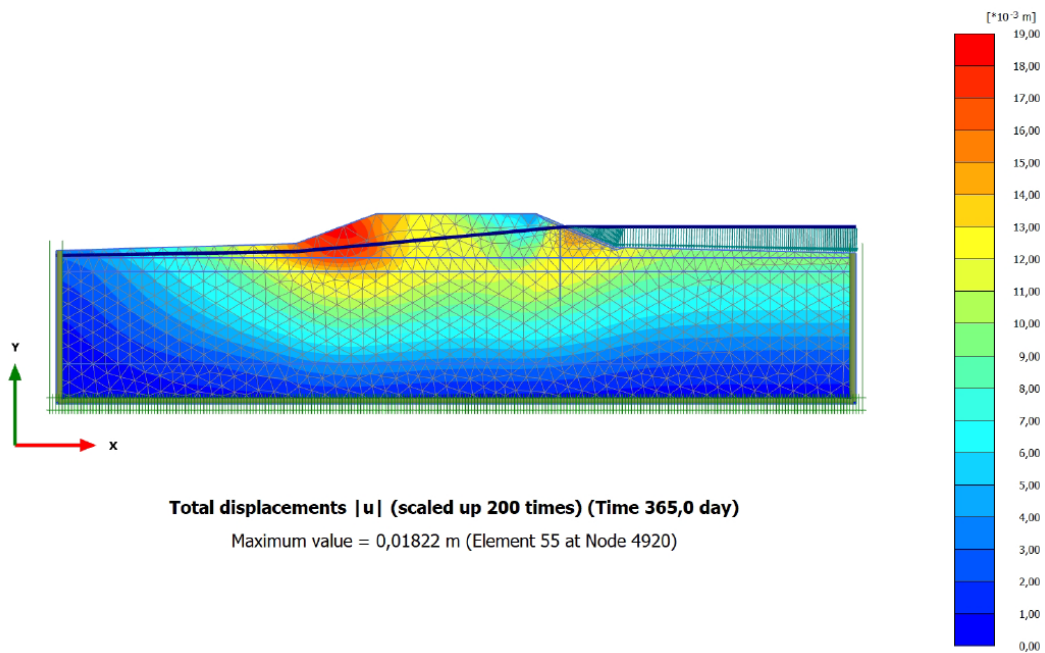


Figure 15: Initial dike model displacements in high water state

Figure 14 indicates the most displacements within the outward slope at the low water state. Adversely, at the high water state (figure 15), inward slope displacements are more present in the model. This phenomenon is due to the rise of the water level, which acts as a counteracting force on the dike. In low water conditions, the soil tends to slide towards the passive side, but

this effect is mitigated in high water conditions. Consequently, the stress distribution shifts towards the hinterland of the dike (Verruijt, 2001).

### 4.3 Critical failure state determination

In the analysis of the safety of the dike model in D-Stability (3.2.5), the landslide effect on the outer slope reveals critical insights concerning the failure mechanism. The safety factor output obtained from PLAXIS retrieves similar results across both states, as shown in the figures 9 and 10.

The figures highlight the most critical effects occurring at the upper section of the slope. Notably, the effects are significantly higher under high water conditions. This leads to the identification of the critical failure state, characterized by the modification of the geometry, as illustrated in the figure below.

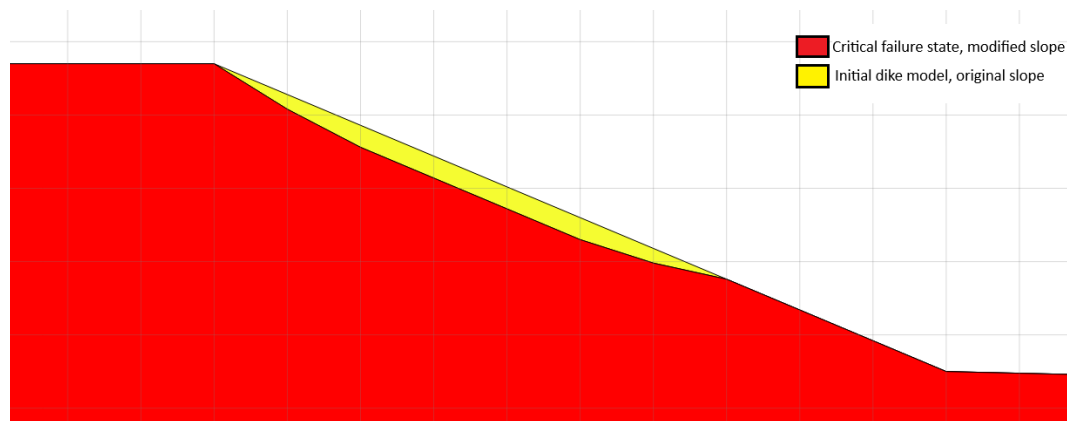


Figure 16: Critical failure state of the model. The slope modification is marked in red, while the original slope is indicated in yellow.

Under the critical failure state, the dike fails when high water level conditions occur. To mitigate this risk, a sheet pile is implemented within the initial dike model as described in figures 14 and 15. The introduction of the sheet pile serves to resist further sliding of the dike while enhancing its overall structural integrity.

### 4.4 Sheet pile implementation

This research focuses on the implementation of the Z-profile sheet pile to mitigate the risk of sliding along the dike, as mentioned in paragraph 3.3. Various Z-profile types are available and are evaluated through simulations. The outcomes of this analysis provide insights into the performance of different sheet pile configurations.

Initially, the influence of sheet pile placement on landslide prevention is investigated. Three locations are examined along the dike's slope, as shown in figure 17. The placements are

located at (1) the edge of the crest, where the slope failure initiates, (2) the middle of the slope failure, and (3) the end of the slope failure. These placements aim to mitigate the landsliding effect (Tantrio and Suhendra, 2023).

Subsequently, the depths of these sheet piles are based on engineering practices, suggesting that one-third of the sheet pile length equals the slope's length and two-thirds should approximately extend this length (Grand Piling, n.d.). The placements and lengths are illustrated in figure 17, with the corresponding results described in table 6. This table includes the calculated safety factor for low and high water conditions in the critical failure state.

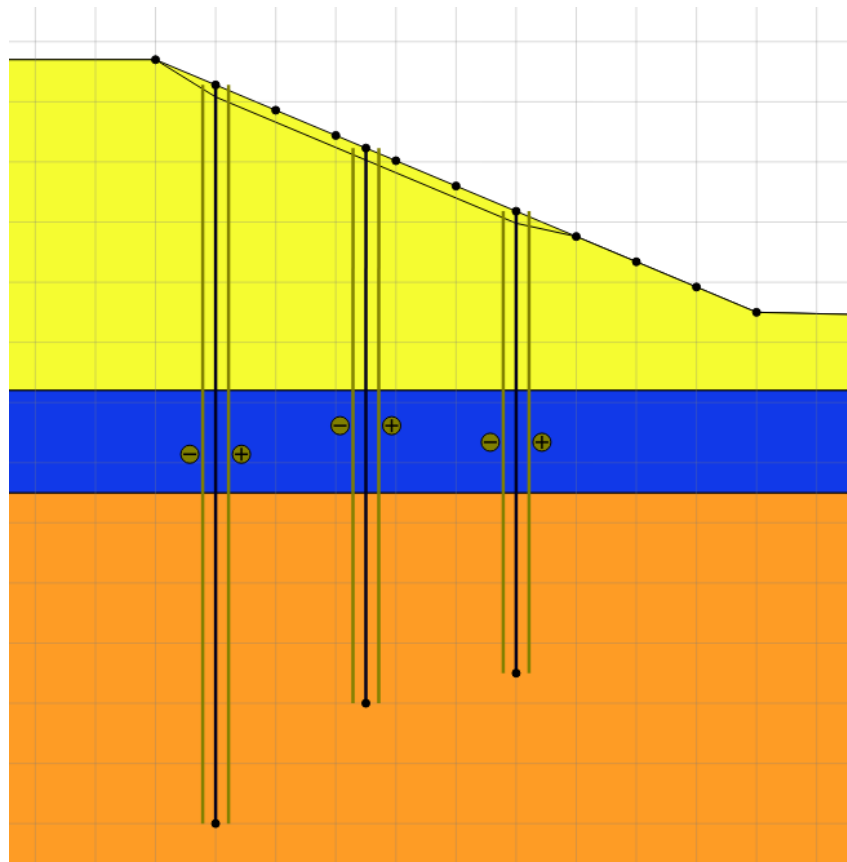


Figure 17: Representation of the sheet pile placements along the slope

<u>Location</u>	<u>Top point [X, Y]</u>	<u>Bottom point [X, Y]</u>	<u>Length [m]</u>	<u>FS High water</u>	<u>FS Low water</u>
Top	61.00 , 8.28	61.00 , -4.00	12.28	1.300	1.290
Middle	63.50 , 7.23	63.5 , -2.00	9.23	1.153	1.155
Bottom	66.00 , 6.18	66.00 , -1.50	7.68	1.027	1.040

Table 6: Results of the three sheet pile placements, including the safety factor calculations in the critical failure state

The results indicate that the best sheet pile placement is at the edge of the crest, considering only the dike’s safety. However, considering economic and sustainability aspects, the bottom point emerges as the optimal choice due to the required sheet pile length. Consequently, this bottom placement is selected for further analysis of various Z-profile sheet piles.

#### 4.4.1 Practical considerations

In engineering practices, sheet pile installations at and around the slope present several advantages and disadvantages. One primary concern is the position of the construction machinery within the inundation area, which is only feasible in low water conditions. Consequently, construction methodologies in this environment are considered and described in the table below (Gilbert Gedeon, 1994).

	Advantage	Disadvantage	Remarks
<b>Accessibility</b>	No hinder of human factors	No roadway present	Consider road plates
<b>Underground</b>	No cables and pipes present in general	Usually wet and soft layers present, making it difficult for the machinery to settle	Consider habitat of animals
<b>Water</b>	-	Prevents a stable settlement for machinery	Consider the soil-water interaction when heavy machinery are applied

Table 7: Construction considerations within the inundation area (Gilbert Gedeon, 1994)

Adversely, the sheet pile installation at the crest of the dike presents different advantages and disadvantages, as shown in table 8.

	Advantage	Disadvantage	Remarks
<b>Accessibility</b>	Roadway present	Part of the traffic must be jammed	Consider speed limitations, traffic controllers, and other human factors
<b>Underground</b>	Hard underground for the machinery to settle	Possible cables and pipes present	Consider the dike’s geometry to assess feasibility
<b>Water</b>	Mostly dry	-	Consider groundwater levels

Table 8: Construction considerations on top of road (Gilbert Gedeon, 1994)

The installation at the crest offers a more stable placement for the construction machinery. Especially, due to the presence of a more stable underground. This placement is integrated into the PLAXIS model to account for the load of the machinery (Gilbert Gedeon, 1994).

Other practical considerations are acoustic and vibrational aspects during construction activities in the surrounding environment. These aspects include monitoring activities to mitigate potential disturbances and are not processed into the model (CUR, 2023).

#### 4.4.2 Evaluation of Z-type sheet piles

Various Z-type sheet piles are evaluated to assess their impact on the structural integrity of the dike. This analysis involves the incorporation of the mechanical properties of the selected sheet piles, which are shown in the table below (ArcelorMittal, 2024; Exley, 2024). The determination of the parameter values is described in paragraph 2.5, and is not considered in the optimization with GrainLearning.

Sheet pile	w [kN/m/m]	EA <sub>1</sub> [kN/m]	EA <sub>2</sub> [kN/m]	EI [kN/m <sup>2</sup> /m]
AZ 12-240	0.9904	2.646E6	132.3E3	38.09E3
AZ 18-240	1.179	3.150E6	157.5E3	71.82E3
AZ 25-240	1.454	3.885E6	194.3E3	109.7E3
AZ 37-700-240	1.776	4.746E6	237.3E3	194.0E3
AZ 46-240	2.287	6.111E6	305.6E3	231.9E3
AZ 50-240	2.531	6.762E6	338.1E3	254.2E3

Table 9: Sheet pile parameter values (ArcelorMittal, 2024; Exley, 2024)

For each sheet pile, a safety factor calculation is executed. This includes calculations with top loading conditions, and the dike model in its critical failure state, as described in 5. The outcomes, shown in the table below, allow the selection of a specific sheet pile.

Sheet pile	FS Low water including top loading	FS High water including top loading	FS Low water in critical failure state including top loading	FS High water in critical failure state including top loading
AZ 12-240	1.253	1.235	1.027	1.040
AZ 18-240	1.241	1.220	1.024	1.043
AZ 25-240	1.240	1.238	1.024	1.043
AZ 37-700-240	1.243	1.224	1.027	1.040
AZ 46-240	1.243	1.224	1.022	1.038
AZ 50-240	1.242	1.225	1.020	1.042

Table 10: Safety factors of each sheet pile across different phases

Table 10 indicates a similarity in safety factor values between different sheet piles. However, it is expected that the AZ 50-240 design yield the highest safety factor due to its superior stiffness characteristics, as shown in table 9. This phenomenon is possible due to the minimum displacements present in the dike model, as illustrated in figures 14 and 15 (Roslan and Ling, 2022). This outcome concludes that the selection of these sheet piles has little impact on the dike's stability. Consequently, the AZ 12-240 configuration is selected as its output produces the highest overall safety factor values.

#### 4.5 Analysis of the dike model including sheet pile implementation

The sheet pile implementation into the dike model improves structural integrity and safety. The safety factor values for low and high water states are enhanced to an acceptable value (above 1.00) within the critical failure state. The figures below show the displacements of the dike model, including sheet pile implementation.

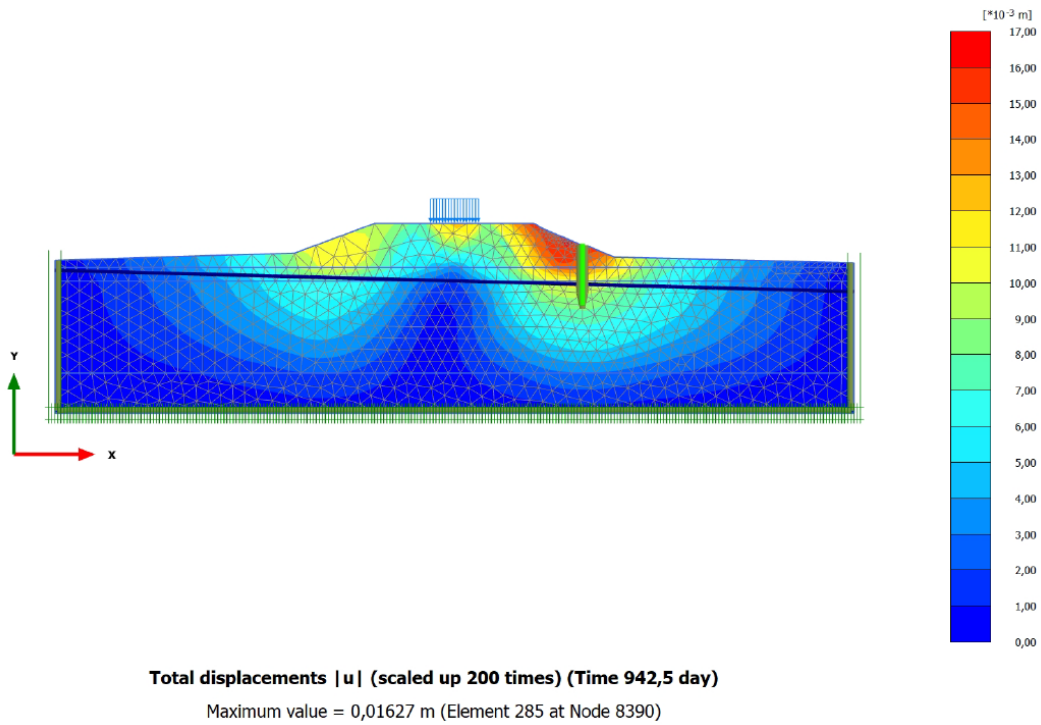


Figure 18: Dike model displacements including sheet pile in low water state (FS = 1.027)

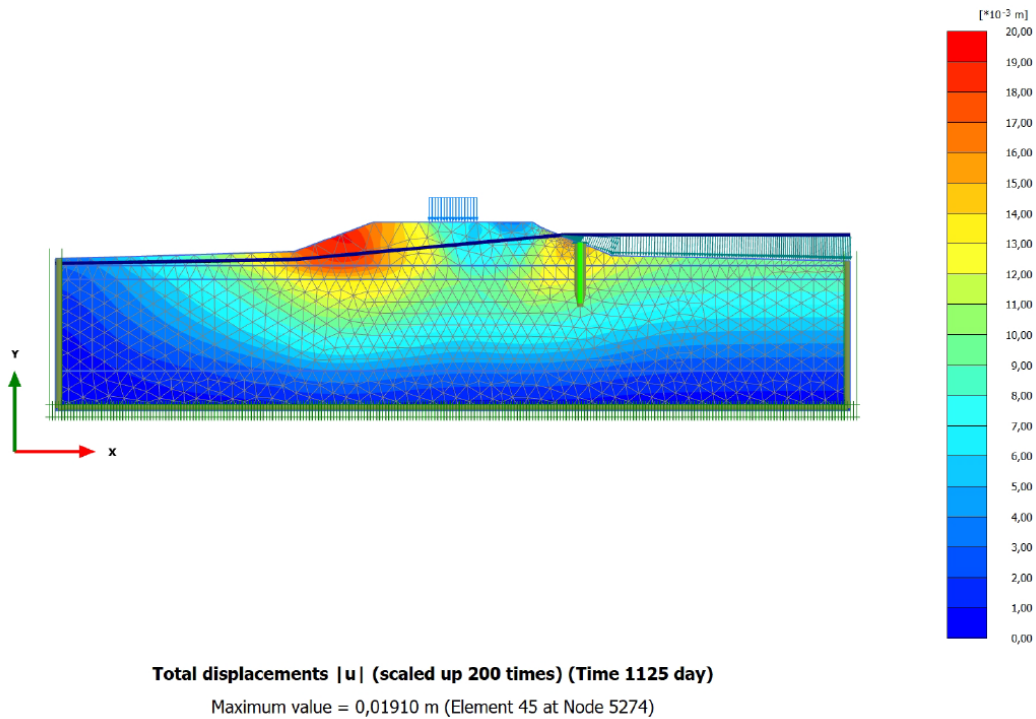


Figure 19: Dike model displacements including sheet pile in high water state (FS = 1.040)

Figure 18 still indicates the presence of the slope circle in low water conditions, as in figure 14. However, the sheet pile implementation mitigates the driving force and ensures the dike's stability, as indicated within the safety factor value (FS = 1.027). Furthermore, the top loadings, in combination with the sheet pile, ensure the stress distribution towards the core and hinterland of the dike (Das, 2010).

The high water state, illustrated in figure 19, indicates a more stable scenario, as shown in the safety factor value (FS = 1.040). The deformations exhibit an inverse behavior, primarily caused by the increased hydraulic pressure on the waterside. The pressures from the riverside act as the active side, while the dike section shifts to the passive side. This phenomenon ensures more vulnerability in the inward slope of the dike (Terzaghi, 1943).

#### 4.6 Initial model used for GrainLearning

The model, shown in figures 18 and 19, is employed as the initial model for the simulations within GrainLearning. The safety factor values obtained in low and high water conditions are used as the reference values throughout the analysis. The objective of this analysis is to achieve a sheet pile configuration that closely approximates the referred safety values while simultaneously minimizing the length as far as possible.

## 5 Results

This section describes the application of GrainLearning and its output. To ensure the integration within PLAXIS, the existing Python script is modified. The Bayesian inference tool executes multiple simulations and tries to identify a shortened sheet pile length (indicated with Y2) that corresponds closely to the safety factor values as described in figures 18 and 19.

Paragraph 2.7 describes the methodology of the GrainLearning tool across different tests. However, with this initial model for GrainLearning established, more clarity on the different tests can be provided.

The results of all tests are shown below with the corresponding probability distributions. The results retrieve a probable value for the sheet pile depth (bottom point Y2) to test in PLAXIS. The sheet pile length is derived from this probable value, where the difference between the top point and bottom point is taken. Subsequently, this sheet pile length corresponds to calculated safety factor values in the critical failure state in low and high water conditions, utilizing PLAXIS.

Furthermore, a ranking system for each test is established to determine the best sheet pile configuration, including safety, economic, and sustainability aspects. The safety ranking (Ranking FS) is determined by the cumulative values of the two safety factor values in low and high water conditions. The sustainability and costs ranking (Ranking S&C) is derived from the total sheet pile length required. The summation of these two rankings yields a score, from which a subsequent ranking (Ranking overall) is generated.

### 5.1 Variation tests

The variation tests consist of a diverse range of iterations and sample combinations to assess the impact of deviations from the initial model, as described in paragraph 2.7.1.

For the simulation of a new sheet pile length in this test, constraints in the minimum and maximum range are established based on geological considerations. The maximum depth is set to 1 meter, which correlates to the presence of a hard layer (moderate sand) below the soft layer (clay, weak) in the dike model. It is important for sheet piles to anchor within a competent layer to mitigate potential settlement and displacements over time (Gilbert Gedeon, 1994).

The minimum depth is derived from engineering practices, suggesting that one-third of the sheet pile length equals the slope's length and two-thirds is approximately the extent of this length (Grand Piling, n.d.). In this case, the length over a meter distance on the slope is used, which equals approximately 0.5 meters. This results in a minimum depth of 1.5 meters below

the slope (0.5 (one-thirds) + 1 (two-thirds)), which for this initial model equals 4.68 meters.

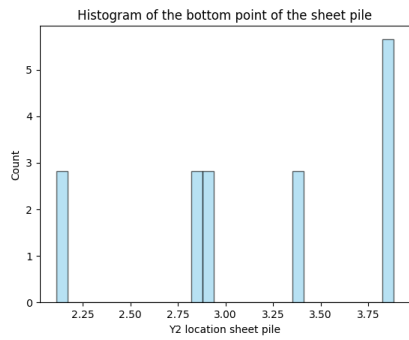
The results from the variation tests are shown in the table below.

<b>Parameter</b>	<b>Value</b>			
Iterations	3	<u>5</u>	8	8
Samples	6	<u>8</u>	8	10
Most probable sheet pile depth (bottom point Y2) [m]	3.856	3.805	4.305	4.305
Most optimal length (sheet pile length) [m]	2.324	2.375	1.875	1.875
FS Low water critical failure state	1.025	1.025	1.026	1.026
FS High water critical failure state	1.037	1.036	1.037	1.037

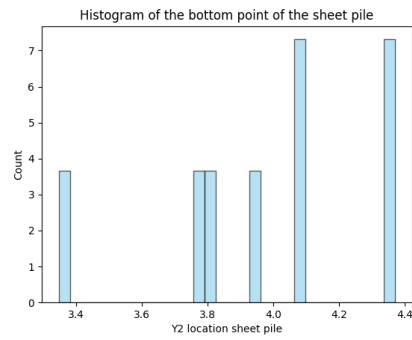
Table 11: Results for the variation tests, with the default parameters highlighted with an underline

The results demonstrate consistent safety factor outputs across all iterations and sample combinations, with a deviation of 0.001. Notably, the variability in these safety factor values in comparison with the initial model, deviates from 0.003 to 0.004. Furthermore, the iterations and sample configurations reveal differences in the amount of iterations utilized. Specifically, between 5 and 8 iterations with both 8 samples, yield a difference of 0.5 meters in the sheet pile length. This variation impacts construction considerations including economic and sustainability aspects of extensive dike trajectories reinforcement.

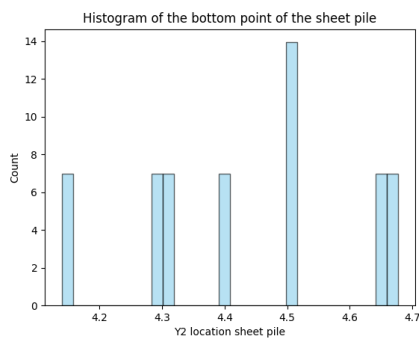
The probability distributions corresponding to the iterations and sample combinations are shown in the figures below.



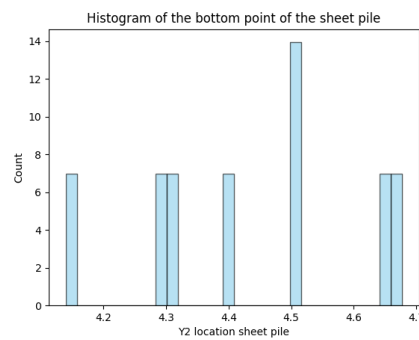
(a) 3 iterations / 6 samples



(b) 5 iterations / 8 samples



(c) 8 iterations / 8 samples



(d) 10 iterations / 8 samples

Figure 20: Variation tests results - results in paragraph 5.1

### 5.1.1 Ranking variation tests

The variation test ranking consists of two distinct approaches, an overall ranking and a ranking that includes the simulation time. The overall ranking, outlined in the table below, excludes the simulation time.

1. Iterations / Samples	2. FS low water	3. FS high water	4. Sum FS (2+3)	5. Ranking FS (4)	6. Sheet pile length	7. Ranking S&C (6)	8. Sum overall (5+7)	9. Ranking overall (8)
3 / 6	1.025	1.037	2.062	3	2.324	3	6	3
5 / 8	1.025	1.036	2.061	4	2.375	4	8	4
8 / 8	1.026	1.037	2.063	1	1.875	1	2	1
8 / 10	1.026	1.037	2.063	1	1.875	1	2	1

Table 12: Ranking of the variation tests for each iteration and sample configuration

The ranking indicates that the simulations with 8 iterations and 8 samples yield the best scores together with the configuration of 8 iterations and 10 samples. However, when including simulation time, the rankings differ, as shown in the table below. Increased iterations and samples require additional computational time. Consequently, the costs are increased due to the required working hours.

1. Iterations / Samples	2. Ranking FS	3. Ranking S&C	4. Simulation time (1)	5. Ranking simulation time (4)	6. Sum all rankings (2+3+5)	7. Ranking incl. simulation time (6)
3 / 6	3	3	18	1	7	3
5 / 8	4	4	40	2	10	4
8 / 8	1	1	64	3	5	1
8 / 10	1	1	80	4	6	2

Table 13: Ranking of the variation tests including the simulation time

This ranking reveals that the optimal iterations and sample combinations are maintained at 8 iterations and 8 samples, while the configuration of 5 iterations and 8 samples scores the lowest.

## 5.2 Location shift tests

The selection of various sheet pile placements is based on the finite element model results, as described in paragraph 2.7.2. Three different placements were evaluated in paragraph 4.4 and proven to influence the safety of the dike. Consequently, various locations along the slope are investigated for this test, as indicated in table 14. The locations are illustrated in the figure below.

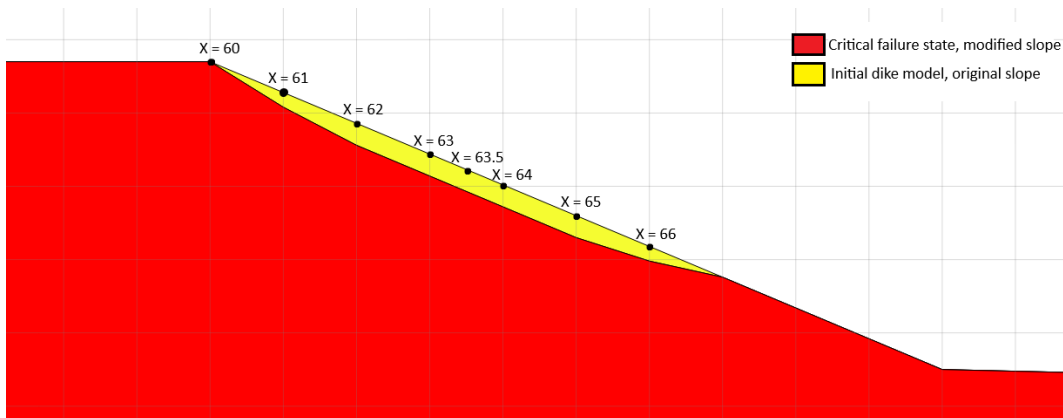


Figure 21: Locations along the dike's slope for investigation

The top point sheet pile refers to the y-coordinate of the structure along the original slope (not the slope in critical failure state). This point corresponds to the x-coordinate along the slope. Consistent with the variation tests for the simulation ranges, the thumb rule is used for the minimum depth, and the maximum depth is set to 1 meter due to the presence of the harder layer. The default parameters are utilized for these tests, consisting of 5 iterations and 8 samples.

<b>Parameter</b>	<b>Value</b>						
Location x-coordinate [m]	60	61	62	63	63.5	64	65
Top point sheet pile y-coordinate [m]	8.7	8.28	7.86	7.44	7.23	7.02	6.6
Min depth for simulation [m]	7.2	6.78	6.36	5.94	5.73	5.52	5.1
Most probable sheet pile depth (bottom point Y2) [m]	1.751	5.372	5.752	3.926	3.906	3.695	3.874
Most optimal length (sheet pile length) [m]	6.949	2.908	2.108	3.514	3.324	3.325	2.726
FS Low water critical failure state	1.025	1.095	1.031	1.027	1.023	1.034	1.026
FS High water critical failure state	1.028	1.094	1.035	1.043	1.035	1.038	1.035

Table 14: Results from the location shift tests

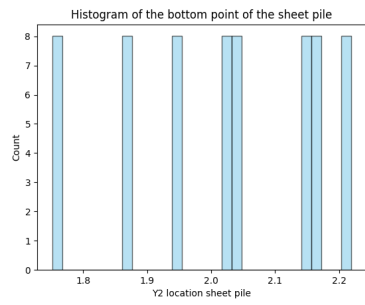
The findings show a diverse range of sheet pile lengths, with the most required length observed at  $X = 60$  which is at the edge of the crest. Additionally, the safety factor values are the least at this location, leading to the least favorable location for sheet pile installation.

The second location ( $X = 61$ ), positioned one meter along the slope from the crest, shows a reduction in the required sheet pile length by 4.041 meters. Furthermore, the safety factor values are improved, with an increase of 0.070 in low-water conditions and 0.066 in high-water conditions.

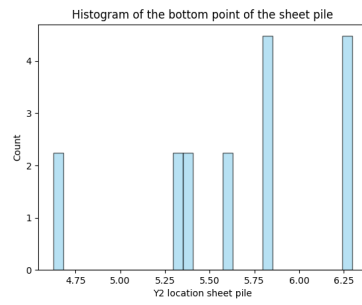
The third location ( $X = 62$ ) further decreases the sheet pile length by 0.80 meters but reduces the safety factor value by 0.064 in low water and 0.059 in high water.

Locations  $X = 63$ ,  $X = 63.5$ , and  $X = 64$  present similar required sheet pile lengths. Notably, location  $X = 63$  yields the highest safety factor values in both conditions. Location  $X = 65$  requires an approximated sheet pile length as  $X = 61$ , but yields safety factor values significantly lower.

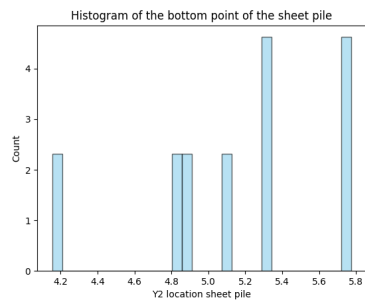
The probability distributions corresponding to the locations are shown in the figures below.



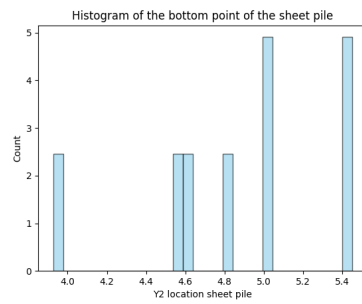
(a)  $X = 60$



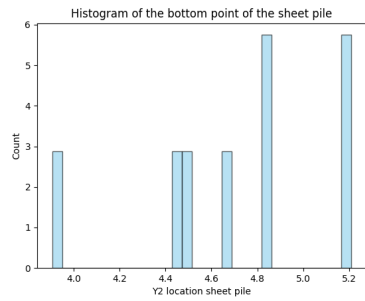
(b)  $X = 61$



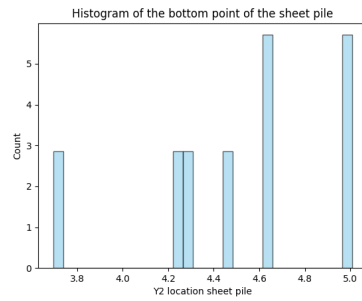
(c)  $X = 62$



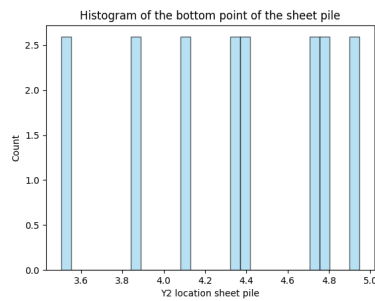
(d)  $X = 63$



(e)  $X = 63.5$



(f)  $X = 64$



(g)  $X = 65$

Figure 22: Location shift tests results - results in paragraph 5.2

### 5.2.1 Ranking location shift tests

The assessment of the location shift tests is based on the safety, sustainability, and cost aspects. Similar to the ranking of the variation tests excluding the simulation time, as shown in table 12. However, the location shift test ranking is ranked on the different locations, while maintaining a consistent number of iterations and samples (5 and 8 respectively).

1. Location x-coordinate [m]	2. FS low water	3. FS high water	4. Sum FS (2+3)	5. Ranking FS (4)	6. Sheet pile length	7. Ranking S&C (6)	8. Sum overall (5+7)	9. Ranking overall (8)
60	1.025	1.028	2.053	7	6.949	7	14	7
61	1.095	1.094	2.189	1	2.908	3	4	1
62	1.031	1.035	2.066	4	2.108	1	5	2
63	1.027	1.043	2.07	3	3.514	6	9	5
63.5	1.023	1.035	2.058	6	3.324	4	10	6
64	1.034	1.038	2.072	2	3.325	5	7	3
65	1.026	1.035	2.061	5	2.726	2	7	3

Table 15: Ranking of the location shift tests for each location [x]

This analysis identifies  $X = 60$  as the optimal placement for the sheet pile installation and is present one meter from the crest on the slope. This location yields the highest safety factor value while achieving a respectable third ranking in sustainability and cost-effectiveness. Only locations  $X = 62$  and  $X = 65$  performed better in the sustainability and cost-effectiveness ranking but presented a respectively fourth and fifth ranking in the safety criteria. Location  $X = 60$  is identified as the least favorable location across all rankings.

### 5.3 Length reduction tests

The execution of this test is described in paragraph 2.7.3. The simulations in previous tests were executed at 1 meter, due to the presence of the harder layer under the clay layer. This depth anchors the sheet pile and mitigates potential settlement and displacements. However, the length reduction tests aims to reduce the required length further by limiting the maximum simulation depth. Specifically, this depth is positioned at 3.20 meters, above the clay layer and is characterized by loose sand, which also can function as a hard layer (CUR, 2023). The outcomes are presented in table 16.

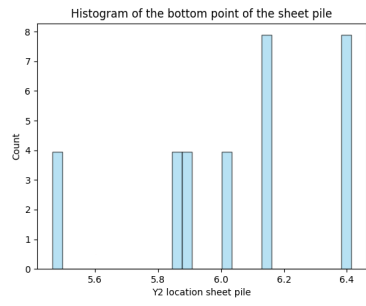
<b>Parameter</b>	<b>Value</b>							
Location	60	61	62	63	63.5	64	65	66
Top point sheet pile [m]	8.7	8.28	7.86	7.44	7.23	7.02	6.6	6.18
Max depth for simulation [m]	7.2	6.78	6.36	5.94	5.73	5.52	5.1	4.68
Most probable sheet pile depth (bottom point Y2)	-	6.415	6.217	5.657	4.742	4.931	4.892	6.365
Most optimal length (sheet pile length) [m]	-	1.865	1.643	1.783	2.488	2.089	1.708	1.815
FS Low water critical failure state	-	1.083	1.021	1.023	1.031	1.023	1.024	1.029
FS High water critical failure state	-	1.092	1.037	1.039	1.035	1.037	1.033	1.035

Table 16: Results from the length reduction tests

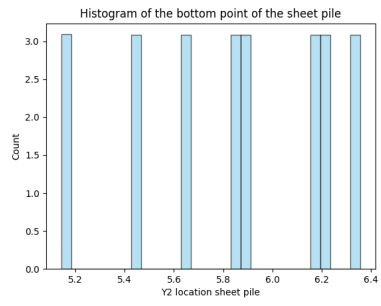
The results indicate that location  $X = 61$  consistently achieves a higher safety factor value compared to other locations. This can be possible due to the configuration of the sliding line, which permits the sheet pile to effectively mitigate the risk of sliding further (Tantrio and Suhendra, 2023).

Location  $X = 60$  reveals that a sheet pile implementation above the clay layer provides no sufficient safety factor value, resulting in dike failure. The remaining locations indicate similar safety factor values approximately to the initial model. However, the locations  $X = 63.5$  and  $X = 64$  require significantly more sheet pile length.

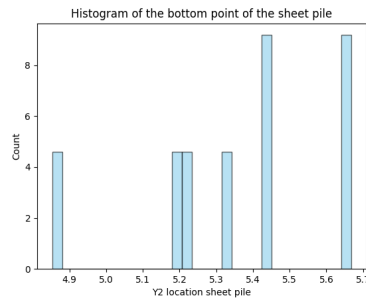
The probability distributions corresponding to the locations are shown in the figures below.



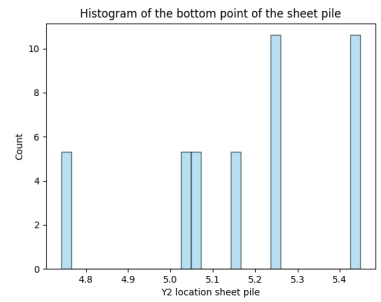
(a)  $X = 61$



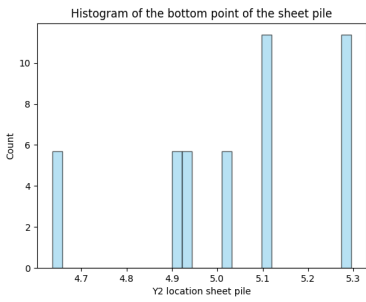
(b)  $X = 62$



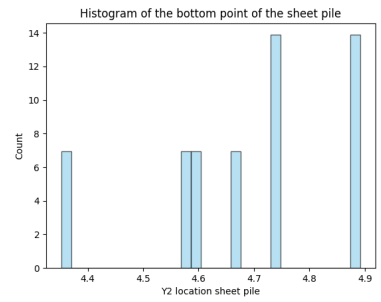
(c)  $X = 63$



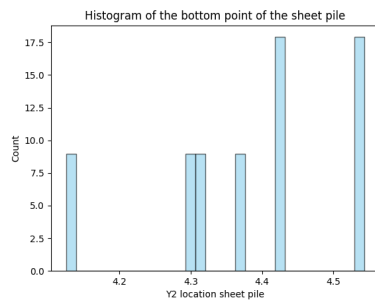
(d)  $X = 63.5$



(e)  $X = 64$



(f)  $X = 65$



(g)  $X = 66$

Figure 23: Length reduction tests results - results in paragraph 5.3

### 5.3.1 Ranking length reduction tests

The ranking of the length reduction tests is similar to the location shift test ranking, as presented in table 15. The results are shown in the table below.

1. Location x-coordinate [m]	2. FS low water	3. FS high water	4. Sum FS (2+3)	5. Ranking FS (4)	6. Sheet pile length	7. Ranking S&C (6)	8. Sum overall (5+7)	9. Ranking overall (8)
60	-	-	-	8	-	8	16	8
61	1.083	1.092	2.175	1	1.865	5	6	1
62	1.021	1.037	2.058	6	1.643	1	7	2
63	1.023	1.039	2.062	4	1.783	3	7	2
63.5	1.031	1.035	2.066	2	2.488	7	9	5
64	1.023	1.037	2.06	5	2.089	6	11	7
65	1.024	1.033	2.057	7	1.708	2	9	5
66	1.029	1.035	2.064	3	1.815	4	7	2

Table 17: Ranking of the length reduction tests for each location [x]

The findings indicate that location  $X = 61$  performs superior to others. This location can achieve the optimized balance in sheet pile design accounting for safety, sustainability, and cost-effectiveness. Conversely, location  $X = 60$  consistently performs the worst across all criteria.

## 5.4 Summary

The findings from the variation tests indicate that the sheet pile length can be minimized by increasing the number of iterations and samples. This approach allows the acquirement of a sufficient safety factor value but increases simulation time. In this research, the optimal combination consists of 8 iterations and 8 samples, together with the configuration of 8 iterations and 10 samples when excluding simulation time. When including simulation time, only the combination of 8 iterations and 8 samples is optimal.

Furthermore, the optimal placement for the sheet pile installation is one meter from the crest of the slope ( $X = 61$ ). The optimal sheet pile length at this location is 1.865 meters and can yield a high safety factor while reducing the sheet pile length significantly.

## 6 Discussion

The results from the variation tests indicate that increasing the number of iterations within the simulation process allows for sheet pile length reduction while maintaining a comparable safety factor value, as shown in table 12. This outcome is important as it addresses sustainability and cost-efficiency aspects in engineering design, depending on location constraints. Specifically, the adjustment from five to eight iterations with eight samples led to a decrease in the sheet pile length of 0.5 meters, offering a preferable alternative without decreasing the dike's safety.

However, the additional iterations increase the simulation time, suggesting the importance of a balanced computational model, specifically when integrating machine learning tools. The limited iteration and sample sizes produce a robust probability distribution, emphasizing the demand for extensive testing. Potentially, hundreds or thousands of trials are required to enhance the certainty and coverage. However, such an approach would require considerable computational time.

The findings of the location shift tests show similar factor of safety values with a significant increase at the optimal placement, but with different sheet pile lengths ranging from 2.108 and 6.949 meters, as shown in table 14. Figure 21 highlights how small shifts in placement along the slope can lead to significant variation in lengths and safety factor values, which underlines the sensitivity of the dike's stability to sheet pile positioning.

This analysis raised the question of whether additional assessment locations should have been considered. This study focuses on assessments at one-meter intervals along the slope to determine the optimal sheet pile design. However, implementing assessments at shorter intervals could potentially yield a more optimal design, possibly allowing for further reduction in length. Therefore, further modifications to the Python script are required to integrate the location shift with the length reduction tests. This approach would enable the machine learning tool to autonomously identify the optimal location and length without implementing specific locations in advance.

Figures 18 and 19 illustrate that the sheet pile implementation mitigates the sliding on the waterside under low and high water conditions at this point of the dike trajectory. This placement occurs near the toe of the dike, which may provide additional protection against various failure mechanisms, such as piping, particularly when installed through the water line. From an engineering and sustainability perspective, such a placement is advantageous as it addresses multiple failure mechanisms at once through a single structural implementation. Consequently, it is important to note that the optimal sheet pile design identified in this research may not fully account for the implications of the piping failure mechanism,

potentially affecting the overall stability of the dike.

Tables 15 and 17 indicate the optimal placement for this case study, one meter from the crest on the slope. Hereby, a sheet pile length of 1.865 meters (table 16) is required to enhance the dike against the macro-stability failure, whose endpoint lies above the water level. This may not be beneficial when assessing the piping failure mechanism. Therefore, a greater length of the sheet pile may be required, but it would negatively affect the economic and sustainability aspects of the design. In this case, the clay layer mitigates the piping mechanism, but this layer may not be as thick as another location of the dike trajectory.

## 7 Conclusion

This study investigates the optimization of sheet pile designs in a sand dike located near the pumping station in Terwolde. The objective is to minimize the sheet pile length while ensuring the dike's safety against external pressures, specifically against outward macro-stability failure. The sheet pile implementation can mitigate this failure mechanism, but requires a safe design. Preferably, a design that also enhances overall sustainability and reduces costs. Such a design would be beneficial for engineering firms, contractors, and the government because it reduces the overall costs and emissions of projects, while also ensuring safety against flooding. Subsequently, this research explores the feasibility of reducing steel usage in sheet pile installations while maintaining the safety and performance of sand dikes.

A PLAXIS model is developed based on location characteristics and loading conditions, which identifies the vulnerability on the outer slope of the dike and the impacts of different hydraulic conditions. Subsequently, the GrainLearning tool was utilized to optimize the sheet pile depth, accounting for safety, sustainability, and cost-effectiveness. Simulations were executed with varying simulation parameters to assess the optimal sheet pile design configuration.

The results indicated that adjusting the simulation parameters can further reduce the sheet pile lengths, yielding a more efficient design. However, computational constraints within PLAXIS necessitate a balanced approach, where a balance between simulation time and output accuracy must be achieved. Further refinement of the maximum depth range for simulations resulted in a better design configuration by a minimized sheet pile length while maintaining acceptable safety factor values. This result requires consideration of whether it is beneficial to increase the engineering time/costs, and potentially reduce the costs and emissions in the construction phase.

The optimized sheet pile design for the sand dike near the pumping station in Terwolde is 1.865 meters long and located one meter from the crest along the slope. These findings proved to be useful in engineering and sustainability practices because the overall length of the sheet pile could be reduced while the engineering time/costs were limited. Also, the corresponding location for the installation of the sheet pile design is achievable during construction due to its level of accessibility.

## 8 Recommendations

For future dike reinforcement projects, the GrainLearning tool can be applied to other geographical locations exhibiting different soil parameters. For instance, regions in the western part of the Netherlands are characterized by clay dikes, which could provide valuable data for analysis. Exploring these locations yields insights into the tool's applicability under varying conditions, allowing a clear evaluation of the tool.

Besides the geographical aspect, the machine learning tool can be developed further technically. One of the improvements is regarding the calibration of the optimal sheet pile design. In this research, the simulation on the location and length reduction of the sheet pile is executed separately, but could be integrated together as one simulation. This approach requires modification of the current Python script and defining boundary conditions depending on the geographical/location characteristics. The boundary conditions are important to let the machine learning tool implement sheet piles along the slope of the dike.

Reassessment of the dike is essential to evaluate the importance of each potential failure mechanism when new construction plans are proposed. This research focuses specifically on the macro-stability failure mechanism, but could be further expanded by including other failure mechanisms, such as piping, overtopping, and settlement. Hereby, other structural implementations can be considered, such as geogrids and CSM-walls. Also, soil improvement aspects can be considered. This expands the tool's possibilities, wherein diverse structural implementations are integrated into the model to strengthen the dike's structural integrity. The goal of such a tool is that it automatically detects the most vulnerable part of the dike, depending on the failure mechanism. Subsequently, it may suggest the structural implementation or soil improvement that is most beneficial regarding safety, costs, and sustainability, where the dike is strengthened against multiple failure mechanisms. Engineering firms, waterboards, or research institutions could make use of such a model.

Other improvements within the machine learning tool are regarding the implementation of the location characteristics in the model. In this research, the dike model was modeled in advance, including the geometry, soil parameters, water levels, and phases. However, not every dike project is similar, and other parameter values are required, which can also be adjusted within the machine learning tool (Python operated). With such a modification, the engineering efficiency can be enhanced even further.

## References

- Abd Alghaffar, M. A., & Dymiotis-Wellington, C. (2004). A life cycle costing model for steel sheet piles incorporating time-dependent reliability. *Int. J. Steel Struct*, 4, 121–129.
- AHN. (2024, August). Ahn-viewer. <https://www.ahn.nl/ahn-viewer>
- ArcelorMittal. (2024, October). Arcelormittal. <https://projects.arcelormittal.com/foundations>
- Arinze, E., & Okafor, C. (2017). Finite element method of stability analysis and stabilization of gully erosion slopes—a study of the otampa gully erosion site, otampa community, isikwuato lga, abia state. *Journal of Civil & Environmental Engineering*, 7.
- Assanangkornchai, S., Tangboonngam, S.-n., & Edwards, J. G. (2004). The flooding of hat yai: Predictors of adverse emotional responses to a natural disaster. *Stress and Health: Journal of the International Society for the Investigation of Stress*, 20(2), 81–89.
- Bentley. (2023). Plaxis 2023.2 material models manual 2d.
- Bijker, W. E. (2007). Dikes and dams, thick with politics. *Isis*, 98(1), 109–123.
- Bobrowsky, P. T., & Marker, B. (2018). *Encyclopedia of engineering geology*. Springer Berlin.
- Bredy, S., & Jandora, J. (2019). Numerical modelling of a diaphragm wall process in karolinka dam. *Int J Sci Basic Appl Res Int J Sci Basic Appl Res*, 48, 93–109.
- Bree van, B., Niemeijer, H., Giessen van der, C., & Hoijinck, R. (2011). *Leidraad waterkerende kunstwerken in regionale waterkeringen* (tech. rep.). STOWA.
- Cheng, H., Orozco, L., Lubbe, R., Jansen, A., Hartmann, P., & Thoeni, K. (2024, April). *GrainLearning: A Bayesian uncertainty quantification toolbox for discrete and continuum numerical models of granular materials* (Version v2.0.3). Zenodo. <https://doi.org/10.5281/zenodo.11001174>
- CUR. (2023). *Damwandconstructies (deel 1 en 2)* (tech. rep.). CROW-CUR.
- Das, B. (2010). *Principles of geotechnical engineering, 7th edition*. Chris Carson/Cengage Learning.
- Deft University of Technology. (2016). Plaxis 2d. *Deft University of Technology & PLAXIS, Netherlands*.
- Douben, K.-J. (2006). Characteristics of river floods and flooding: A global overview, 1985–2003. *Irrigation and Drainage: The journal of the International Commission on Irrigation and Drainage*, 55(S1), S9–S21.
- Exley, B. (2024, June). Plaxis 3d: Geotechnical engineering software: Bentley systems. <https://www.bentley.com/software/plaxis-3d/>
- Fohl, F., & Hechler, O. (2023). Reuse of steel sheet piles—best practice. In *Creating a roadmap towards circularity in the built environment* (pp. 25–35). Springer Nature Switzerland Cham.
- Gilbert Gedeon, P. (1994). Design of sheet pile walls. *US Army Corps of Engineers, Washington, DC*.

- Grand Piling. (n.d.). Sheet pile wall. <https://www.china-steel-piling.com/news/sheet-pile-wall-104.html>
- Greaves, G. N., Greer, A. L., Lakes, R. S., & Rouxel, T. (2011). Poisson's ratio and modern materials. *Nature materials*, *10*(11), 823–837.
- Hoekstra, A. Y., & De Kok, J.-L. (2008). Adapting to climate change: A comparison of two strategies for dike heightening. *Natural hazards*, *47*, 217–228.
- Kahlström, M. (2013). Plaxis 2d comparison of mohr-coulomb and soft soil material models.
- Laera, A., Miranda, V., Azeiteiro, R., Bui, T., Brasile, S., & Brinkgreve, R. (2024). Finite element modelling of a tailings dam using the clay and sand model. In *Geotechnical engineering challenges to meet current and emerging needs of society* (pp. 1712–1717). CRC Press.
- Levasseur, S., Malécot, Y., Boulon, M., & Flavigny, E. (2008). Soil parameter identification using a genetic algorithm. *International journal for numerical and analytical methods in geomechanics*, *32*(2), 189–213.
- Linnemann, Y. (2024, March). Inferring the permeability field under embankments using hydraulic head measurements.
- Liu, Y. (2013). Effects of mesh density on finite element analysis. *SAE Technical Papers*, *2*. <https://doi.org/10.4271/2013-01-1375>
- Maatkamp, T. (2016, October). The capabilities of the plaxis shotcrete material model for designing laterally loaded reinforced concrete structure in the subsurface.
- Macciotta, R. (2018). Shear stress. In P. T. Bobrowsky & B. Marker (Eds.), *Encyclopedia of engineering geology* (pp. 833–833). Springer International Publishing. [https://doi.org/10.1007/978-3-319-73568-9\\_258](https://doi.org/10.1007/978-3-319-73568-9_258)
- Nanjing Grand Steel Piling Co.,Ltd. (2024, October). Stalen-damwand. <https://www.stalen-damwand.nl/>
- Narvaez, L. B. (2020). Analyse berekening stabiliteit buitenwaarts van regionale keringen.
- NEN. (2017). *Nen 9997-1+c2 geotechnical design of structures* (tech. rep.). Nederlandse norm.
- Pantev, I., & Rutgers, A. (2022). *Zoutkamp - integrale vervormingsanalyse bouwkuipen gemaal en sluisbreiding* (tech. rep.). CRUX Engineering BV.
- Pham, Q. V., Nguyen, T. T. T., Phu, N. T., & Le, T. P. (2024). Assessing dike sliding risk due to seasonal water level changes. In N. T. Hai, N. X. Huy, K. Amine, & T. D. Lam (Eds.), *Eai international conference on renewable energy and sustainable manufacturing* (pp. 69–83). Springer Nature Switzerland.
- PLAXIS. (2015). *Material models manual* (tech. rep.).
- Rippi, A., Nuttall, J., Teixeira, A., & Schweckendiek, T. (2016). Reliability analysis of a dike with retaining wall using fem. *6th Asia-Pacific Symposium on Structural Reliability and its Applications (APSSRA6)*.

- Roslan, A., & Ling, F. N. L. (2022). Comparative study of the steel sheet pile wall with concrete and polymer sheet pile wall. *Recent Trends in Civil Engineering and Built Environment*, 3(1), 1656–1664.
- Sasse, J. (2023). *Gemaal terwolde, definitief ontwerp - nieuwe gemaal* (tech. rep.). Nepocon.
- STOWA. (2007). Grip op kwaliteit visuele waarnemingen, verbetering inspectie waterkeringen.
- Tantrio, A., & Suhendra, A. (2023). Analysis of sheet pile position influence in countermeasure to landslide at the cutting slope in infrastructure project. *IOP Conference Series: Earth and Environmental Science*, 1169(1), 012020.
- Terzaghi, K. (1943). *Theoretical soil mechanics*.
- Tu, P. Q., & van Gelder, P. (2013). Stability analysis of the red river dike: The past to the present. *Future*, 2(14.9), 16.
- Van, M., Rosenbrand, E., Tourment, R., Smith, P., & Zwanenburg, C. (2022). Failure paths for levees.
- van Adrichem, S. (2021). Master thesis influence of rapid drawdown on dike stability.
- van Dongen, N. (2023, July). The influence of the numerical approach on pre-augering on sheet pile design. <http://essay.utwente.nl/96636/>
- van Hoven, A., Hardeman, B., van der Meer, J. W., & Steendam, G. J. (2010). Sliding stability of landward slope clay cover layers of sea dikes subject to wave overtopping. *Coastal Engineering Proceedings*, (32), 5–5.
- Van Hoven, A., Den Haan, E., & Rozing, A. (2014). *Residual dike strength after macro-instability* (tech. rep.). WTI2017. Technical report, Deltares, Delft, The Netherlands.
- Verruijt, A. (2001). *Soil mechanics*. Delft University of Technology Delft.
- Visser, P. J. (1999). Breach erosion in sand-dikes. In *Coastal engineering 1998* (pp. 3516–3528).
- Warmink, J. J. (2023, February). Course reader hydraulic engineering.
- Water in Polder Nijbroek. (n.d.). Historie van het gemaal terwolde. <https://waterinpoldernijbroek.nl/historie-van-het-gemaal-terwolde/>
- Yamaguchi, K., Adachi, H., & Takakura, N. (1998). Effects of plastic strain and strain path on young's modulus of sheet metals. *Metals and Materials*, 4, 420–425.
- Yin, Z.-Y., Jin, Y.-F., Shen, J. S., & Hicher, P.-Y. (2018). Optimization techniques for identifying soil parameters in geotechnical engineering: Comparative study and enhancement. *International Journal for Numerical and Analytical Methods in Geomechanics*, 42(1), 70–94.
- Yu, M.-H. (2023). *Soil mechanics: New concept and theory*. Springer Nature.